bioRxiv preprint doi: https://doi.org/10.1101/2020.06.07.138933; this version posted June 7, 2020. The copyright holder for this preprint (which was not certified by peer review) is the author/funder, who has granted bioRxiv a license to display the preprint in perpetuity. It is made available under aCC-BY 4.0 International license.

Environmental conditions dictate differential evolution of vancomycin resistance in *Staphylococcus aureus*

Henrique Machado[a], Yara Seif[a], George Sakoulas[b], Connor A. Olson[a], Richard Szubin[a], Bernhard O. Palsson[a,b,c], Victor Nizet[b,c], Adam M. Feist[a,d,*]

[a] Department of Bioengineering, University of California San Diego, La Jolla, California, USA

[b] Collaborative to Halt Antibiotic-Resistant Microbes, Department of Pediatrics, University of California San Diego, La Jolla, California, USA

[c] Skaggs School of Pharmacy and Pharmaceutical Sciences, University of California San Diego, La Jolla, California, USA

[d] Novo Nordisk Foundation Center for Biosustainability, Technical University of Denmark, Lyngby, Denmark

Running title: *S. aureus'* vancomycin resistant mechanisms

*Address correspondence to Adam M. Feist, afeist@ucsd.edu.

Keywords: adaptive laboratory evolution, *Staphylococcus aureus*, antibiotic resistance, vancomycin, USA300, resistance mechanism, MRSA

bioRxiv preprint doi: https://doi.org/10.1101/2020.06.07.138933; this version posted June 7, 2020. The copyright holder for this preprint (which was not certified by peer review) is the author/funder, who has granted bioRxiv a license to display the preprint in perpetuity. It is made available under aCC-BY 4.0 International license.

Abstract

While microbiological resistance to vancomycin in *Staphylococcus aureus* is rare, clinical vancomycin treatment failures are common, and methicillin-resistant *S. aureus* (MRSA) strains isolated from patients after prolonged vancomycin treatment failure remain susceptible. Adaptive laboratory evolution was utilized to uncover mutational mechanisms associated with MRSA vancomycin resistance in a bacteriological medium used in clinical susceptibility testing and a physiological medium. Sequencing of resistant clones revealed shared and media-specific mutational outcomes, with an overlap in cell wall regulons (*walKRyycHI, vraSRT*). Evolved strains displayed similar genetic and phenotypic traits to resistant clinical isolates. Importantly, resistant phenotypes that developed in physiological media did not translate into resistance in bacteriological media. Further, a bacteriological media-specific mechanism for vancomycin resistance enabled by a mutated *mprF* was confirmed. This study bridges the gap of understanding between clinical and microbiological vancomycin resistance in *S. aureus* and expands the number of allelic variants that result in vancomycin resistance phenotypes.

bioRxiv preprint doi: https://doi.org/10.1101/2020.06.07.138933; this version posted June 7, 2020. The copyright holder for this preprint (which was not certified by peer review) is the author/funder, who has granted bioRxiv a license to display the preprint in perpetuity. It is made available under aCC-BY 4.0 International license.

Introduction

Antibiotic resistance is a global healthcare threat worldwide (Organization, 2014; (u.s.) and Centers for Disease Control and Prevention (U.S.), 2019). Consequently, numerous strategies have been developed and implemented to monitor, assess, and circumvent the development of antibiotic resistance among pathogens (Alcock et al., 2020; Martens and Demain, 2017; Pollack and Srinivasan, 2014). Continual monitoring and assessment are key to getting a global picture of the problem and increasing our understanding of the mutational mechanisms that pathogens employ towards resistance development.

Although somewhat successful, current monitoring and assessment approaches are based on existing pathogen-specific knowledge. Because mechanisms for antibiotic resistance evolution are poorly defined, full realization of critical threats often occurs only after resistance has emerged. Importantly, the evaluation of allelic variations known to lead to reduced susceptibility to a given antibiotic do not account for all the other variations of that same allele or variation in other alleles that can result in the same phenotype (Mitsakakis et al., 2018). Furthermore, bacterial susceptibility to antibiotics is measured following guidelines of the Clinical & Laboratory Standards Institute (CLSI), which recommend using the bacteriological rich media cation-adjusted Mueller-Hinton broth (CA-MHB) to determine antibiotic susceptibility. CA-MHB was specifically developed for its ability to reliably support the cultivation of common human pathogens from clinical samples, and only later adopted for minimum inhibitory/bactericidal concentration (MIC/MBC) testing of antibiotic candidates. However, CA-MHB does not come close to recapitulating the environment encountered by bacteria *in vivo* and has been shown to be less reliable in predicting *in vivo* activity of antibiotics than other more physiological

bioRxiv preprint doi: https://doi.org/10.1101/2020.06.07.138933; this version posted June 7, 2020. The copyright holder for this preprint (which was not certified by peer review) is the author/funder, who has granted bioRxiv a license to display the preprint in perpetuity. It is made available under aCC-BY 4.0 International license.

media such as mammalian tissue culture media (Ersoy et al., 2017; Farha et al., 2018; Kumaraswamy et al., 2016). Adaptive laboratory evolution (ALE) is a strategy that allows the investigator to address both the issues of limited coverage of allelic variation and environment-specific susceptibility through the study of identification of causal mutational mechanisms(Dragosits and Mattanovich, 2013; Mohamed et al., 2017; Salazar et al., 2020). ALE leverages microbial growth under different environments and conditions, wherein the natural mutation rate of bacteria can be exploited to sample successful allelic variations.

Staphylococcus aureus is a historical example of the successful development of antibiotic resistance by a common human pathogen, with methicillin-resistant strains (MRSA) presenting significant treatment challenges (Howden et al., 2010; Mwangi et al., 2007; Pader et al., 2016). The most commonly recommended drug for the treatment of MRSA infections is the glycopeptide vancomycin (Sorrell et al., 1982). Even though very few vancomycin-resistant MRSA clinical isolates have been reported (Hidayat et al., 2006; Hiramatsu et al., 1997; Howe et al., 1998), an increasing challenge of clinical treatment failures is well documented (Howden et al., 2010). The established MIC breakpoints determined by CLSI classify *S. aureus* into three susceptibility categories: vancomycin-susceptible *S. aureus* (VSSA, MIC ≤ 2 μg/mL), vancomycin intermediate-resistant *S. aureus* (VISA, MIC = 4-8 μg/mL), and vancomycin-resistant *S. aureus* (VRSA, MIC ≥ 16 μg/mL).

Here we used a clinical MRSA isolate (TCH1516) and applied adaptive laboratory evolution to uncover mutational mechanisms associated with resistance under two

bioRxiv preprint doi: https://doi.org/10.1101/2020.06.07.138933; this version posted June 7, 2020. The copyright holder for this preprint (which was not certified by peer review) is the author/funder, who has granted bioRxiv a license to display the preprint in perpetuity. It is made available under aCC-BY 4.0 International license.

different environmental conditions: (i) CA-MHB, the nutrient rich bacteriological medium used for clinical susceptibility testing by CLSI recommendations; and (ii) Roswell Park Memorial Institute medium (RPMI), a mammalian cell culture medium that better mimics human physiology (McKee and Komarova, 2017). We further phenotypically characterized several vancomycin-tolerant and -resistant clones and identified genetic mutations responsible for such adaptations. The mutational evolutionary pathways towards vancomycin tolerance exhibited media specificity, with an overlap in regulatory rearrangements in cell wall regulons. We also establish that vancomycin-resistant phenotypes that developed in physiological media do not translate into resistance in bacteriological media, where a major resistance mechanism relies on change of the cell surface charge by mutation of *mprF*. This study significantly expands knowledge of allelic variation that contributes to *S. aureus* vancomycin tolerance.

bioRxiv preprint doi: https://doi.org/10.1101/2020.06.07.138933; this version posted June 7, 2020. The copyright holder for this preprint (which was not certified by peer review) is the author/funder, who has granted bioRxiv a license to display the preprint in perpetuity. It is made available under aCC-BY 4.0 International license.

Results

Tolerization of *S. aureus* TCH1516 to vancomycin. Adaptive Laboratory Evolution (ALE) relies on the natural capability of cells to adapt to new environments. Here, we have applied this technology to engender tolerance of *S. aureus* TCH1516 to vancomycin, and unravel the molecular mechanisms for this adaptation, in a so-called Tolerization ALE (TALE) (Mohamed et al., 2017; Salazar et al., 2020). Two media types were used in this experiment: CA-MHB, an undefined defined nutrient rich bacteriological medium used for clinical susceptibility testing and the well-defined Roswell Park Memorial Institute medium (RPMI), routinely used in the culturing of mammalian cells, and which resembles the physiological conditions in the human body (McKee and Komarova, 2017), supplemented with 10% bacteriological rich Luria-Bertani medium (RPMI+) to ensure bacterial growth equivalency. For each media type, four replicates of wild-type (WT) and of two media-adapted clones were evolved to stepwise increasing concentrations of vancomycin (Figure 1A). The TALE experiments were conducted for ~30 days and ~$5x10^{12}$ cumulative cell divisions (CCDs). The final vancomycin concentrations reached an average of 5.14 ± 0.46 μg/mL in CA-MHB and 6.13 ± 1.03 μg/mL in RPMI+ (Figure 1B), compared to a tenth of the MIC used as start concentration (MIC in Supplementary Table 1; starting concentration of 0.1 and 0.2 μg/mL, in CA-MHB and RPMI+ TALEs, respectively).

bioRxiv preprint doi: https://doi.org/10.1101/2020.06.07.138933; this version posted June 7, 2020. The copyright holder for this preprint (which was not certified by peer review) is the author/funder, who has granted bioRxiv a license to display the preprint in perpetuity. It is made available under aCC-BY 4.0 International license.

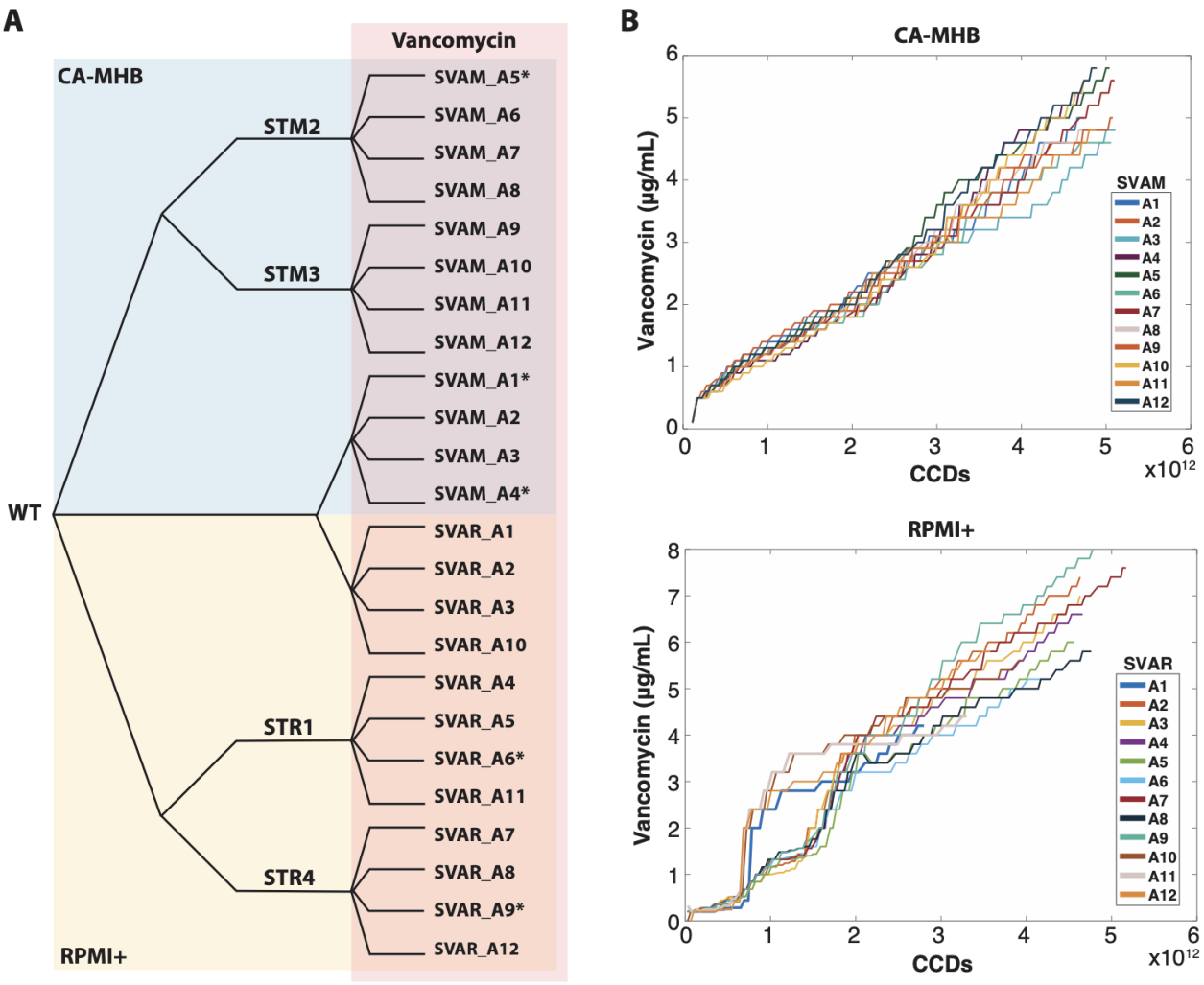

Figure 1. Tolerization Adaptive Laboratory Evolution. (A) Experimental design. Wild-type (WT) *S. aureus* TCH1516 was used as starting strain along with strains which were initially adapted to each media condition (Salazar et al., 2020). Strains were tolerized under CA-MHB (blue) and RPMI+ (yellow) media conditions with increasing concentrations of vancomycin (red). Isolate naming from each lineage is listed. (B) Plots showing the stepwise increase of vancomycin throughout the TALE experiments. * denotes hyper-mutators. STM: *Staphylococcus aureus* adapted to CA-MHB. STR: *Staphylococcus aureus* adapted to RPMI+. SVAM: *Staphylococcus aureus* tolerized to

bioRxiv preprint doi: https://doi.org/10.1101/2020.06.07.138933; this version posted June 7, 2020. The copyright holder for this preprint (which was not certified by peer review) is the author/funder, who has granted bioRxiv a license to display the preprint in perpetuity. It is made available under aCC-BY 4.0 International license.

vancomycin in CA-MHB. SVAR: *Staphylococcus aureus* tolerized to vancomycin in RPMI+. CCDs: cumulative cell divisions.

Phenotypes and tradeoffs in vancomycin tolerization. The TALE evolved strains, adapted for growth in increasing concentrations of vancomycin, were evaluated for changes to their growth phenotypes and antibiotic susceptibility. Growth rate was not affected in TALE strains, but an increase in the lag phase could be identified in CA-MHB-evolved strains when measured with no vancomycin stress and compared to their pre-evolved counterparts (Figure 2A). As expected, TALE strains grew in higher concentrations of vancomycin, with an increase in MIC of up to 8-fold (Supplementary Table 1). Previous studies have outlined the phenotypic characteristics of clinically isolated vancomycin-tolerant strains (Howden et al., 2010; Ishii et al., 2015). We observed similar characteristics in the TALE-evolved strains, including lower hemolytic activity and reduced autolysis (Supplementary Figure 1A and 1B). Further, vancomycin-tolerant strains generated in the laboratory have been reported to be phenotypically unstable (Gardete et al., 2012), losing their tolerance after growth in non-selective conditions. Therefore, we grew the vancomycin-tolerized strains for 21.79 ± 2.08 passages ($9.41 \times 10^{11} \pm 9.84 \times 10^{10}$ CCDs) in the media used for evolution, without vancomycin. The endpoint strains were generally stable in maintaining their tolerance phenotype in 11 out of 12 lineages, with the exception of the SVAM_A10 lineage, which decreased its MIC from 8 to 2 µg/mL (Supplementary Table 1).

bioRxiv preprint doi: https://doi.org/10.1101/2020.06.07.138933; this version posted June 7, 2020. The copyright holder for this preprint (which was not certified by peer review) is the author/funder, who has granted bioRxiv a license to display the preprint in perpetuity. It is made available under aCC-BY 4.0 International license.

TALE strains lost vancomycin susceptibility, with a corresponding increase in their MIC (Supplementary Table 1). We further assessed if this decrease in susceptibility held true across the different media environments. Although CA-MHB vancomycin-tolerized strains (i.e., SVAM) maintained their tolerance phenotypes in RPMI+, the same was not true for the clones evolved in RPMI+. RPMI+ vancomycin-tolerized strains (i.e., SVAR) did not show decreased susceptibility when screened in CA-MHB media (Figure 2B). Thus, the strains evolved under RPMI+ displayed a media-specific tolerance phenotype, as compared to the translatable phenotype of the CA-MHB derived strains, for the two media conditions tested here.

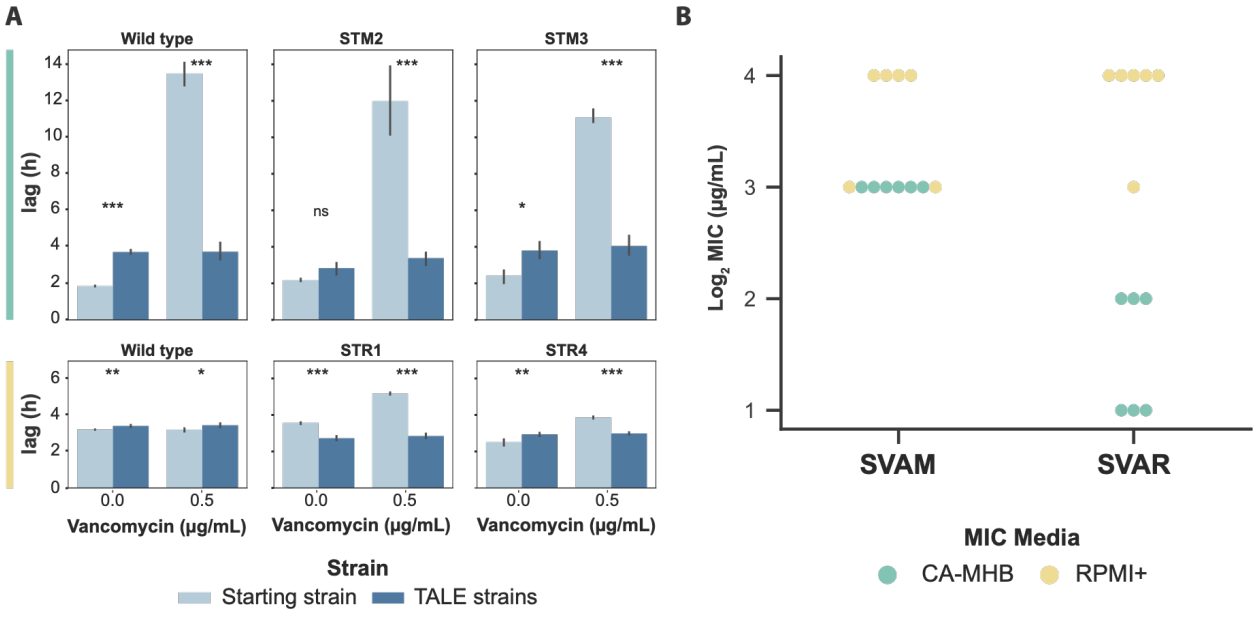

Figure 2. Phenotypic changes observed in vancomycin-tolerized strains. (A) Bar plots displaying growth trade offs grouped by the starting strain for each set of TALE experiments. Evolution starting strains and vancomycin adapted strains were grown in the absence and presence of vancomycin. Assessment of the lag-phase duration of starting strains and evolved strains in the same media as that used for tolerization, CA-

bioRxiv preprint doi: https://doi.org/10.1101/2020.06.07.138933; this version posted June 7, 2020. The copyright holder for this preprint (which was not certified by peer review) is the author/funder, who has granted bioRxiv a license to display the preprint in perpetuity. It is made available under aCC-BY 4.0 International license.

MHB (top, green) and RPMI+ (bottom, yellow). Evolved strain averages used 2, 3 or 4 distinct clones derived from the given starting strain (Supplementary Table 1), all determinations were made in triplicate. Values that are significantly different by ANOVA are indicated by asterisks (ns, non-significant; *, $P \leq 0.05$; **, $P \leq 0.01$; and ***, $P \leq 0.001$) (Supplementary Table 2). (B) A plot of Log_2 vancomycin MIC values of evolved strains from all TALE conditions tested in both media types. SVAR strain tolerance phenotypes did not translate when tested for MIC in CA-MHB media. SVAM: *Staphylococcus aureus* tolerized to vancomycin in CA-MHB. SVAR: *Staphylococcus aureus* tolerized to vancomycin in RPMI+.

Environment dependent mutational strategies to vancomycin tolerization. For each of the 24 independent adaptive evolutionary lineages, 2-3 clones were randomly selected at different time points of the TALE experiments and were sequenced for mutational analysis. For each media type, approximately 400 unique mutations could be identified (462 in CA-MHB and 374 in RPMI+, n=50) (Supplementary Tables 3 and 4), with the majority (approx. 85%) being single nucleotide polymorphisms (SNPs). The percentage of transitions and transversions was quite similar (55% transitions, 45% transversions), but there was a bias in mutations from GC to AT, which constituted about 40% of the SNPs compared to 20% from AT to GC. The observed AT biased mutation has been shown to be universal for bacteria, independently of their genomic GC content (Hershberg, 2015; Hershberg and Petrov, 2010; Hildebrand et al., 2010).

bioRxiv preprint doi: https://doi.org/10.1101/2020.06.07.138933; this version posted June 7, 2020. The copyright holder for this preprint (which was not certified by peer review) is the author/funder, who has granted bioRxiv a license to display the preprint in perpetuity. It is made available under aCC-BY 4.0 International license.

184 Key mutated genes were considered to be those mutated in two or more
185 independent TALE lineages and that were present in at least one clonal sample. If a gene
186 was mutated in multiple flasks of the same TALE lineage or was only observed in
187 sequenced population samples, it was not considered. A total of 69 key mutations were
188 identified for both media types (Supplementary Figure 2). Overall, clones evolved in
189 RPMI+ typically had a lower number of mutations (7.4 ± 3.4 mutations per strain)
190 compared to the ones evolved in CA-MHB (10.6 ± 4.6 mutations per strain), excluding
191 hyper-mutators. This mutational count difference is also reflected in the number of key
192 mutated genes identified in both conditions, 54 versus 26 in CA-MHB and RPMI+,
193 respectively (Figure 3A). By increasing the threshold of lineages with a given gene
194 mutated, the decrease in the number of key mutated genes in CA-MHB was striking,
195 whereas in RPMI+ there was less variance (Figure 3A). Although the *apt* gene appears
196 as a key mutation in RPMI+ because it was mutated in all four replicates that were started
197 from wild-type, this mutation has been associated with a growth rate increase in RPMI+
198 and does not have an effect on antibiotic susceptibility (Salazar et al., 2020). Furthermore,
199 mutations in *mutL* were found in TALE strains from both media conditions and similarly,
200 these strains displayed hypermutator phenotypes similar to previous reports (Ban and
201 Yang, 1998; Glickman and Radman, 1980). The hypermutator strains had a higher
202 number of mutations, compared to other TALE strains. However, the mutations identified
203 were not distinctly linked with vancomycin tolerance but randomly spread throughout the
204 genome (Supplementary Tables 3 and 4).
205

bioRxiv preprint doi: https://doi.org/10.1101/2020.06.07.138933; this version posted June 7, 2020. The copyright holder for this preprint (which was not certified by peer review) is the author/funder, who has granted bioRxiv a license to display the preprint in perpetuity. It is made available under aCC-BY 4.0 International license.

206 Distinct key mutations were identified in both bacteriological and physiological
207 media conditions, with the overlap of similar mutations being mostly in regulatory genes,
208 specifically in the *vra* and *wal* regulatory systems (Figure 3A). Mutations in these two
209 systems have been previously associated with decreased susceptibility to glycopeptides
210 (Gardete et al., 2012; Howden et al., 2010; Hu et al., 2016; Kato et al., 2010). For the *vra*
211 system, comprised of the genes *vraSRT*, we identified 37 different mutations, of which 5
212 exact mutations (VraT-A151T, VraS-A314V, VraS-G88D, VraS-T264A, and VraR-V14I)
213 and 2 mutated positions (VraT-P126 and VraT-N74) have been previously described
214 (Cameron et al., 2012; Hu et al., 2016; Kato et al., 2010). For the *wal* system, comprising
215 genes *walKRyycHI*, we identified 44 mutations, 26 of which were in the accessory genes
216 *yycHI* (21 resulting in possible pseudogenization, i.e. gene disruption). This
217 pseudogenization type of gene disruption (specifically, a frameshift mutation resulting in
218 truncation) had been previously observed in an *in vivo* evolution study in a patient
219 (Mwangi et al., 2007). From the 18 mutations in *walKR*, only one mutated position has
220 been previously described (WalK-G223), which in previous studies resulted in an amino
221 acid substitution at position 223 from glycine to aspartic acid (Howden et al., 2011; Hu et
222 al., 2015; Vidaillac et al., 2013), and in our case to alanine. The alleles mutated strongly
223 correlate with the ones found in clinical isolates, although most of the specific mutations
224 are different, contributing to an expansion of the tolerance alleleome.
225
226 Vancomycin targets the cell wall, therefore, the finding that most of the key mutated
227 genes under both TALE media conditions were related to cell wall biosynthesis was
228 expected (i.e., *sgtB, prsA, walKRyycHI, vraSRT, pbp2, murJ_2, mprF*)(Hiramatsu, 2001;

bioRxiv preprint doi: https://doi.org/10.1101/2020.06.07.138933; this version posted June 7, 2020. The copyright holder for this preprint (which was not certified by peer review) is the author/funder, who has granted bioRxiv a license to display the preprint in perpetuity. It is made available under aCC-BY 4.0 International license.

Jousselin et al., 2015; Kuroda et al., 2003; Łęski and Tomasz, 2005; Oku et al., 2004; Villanueva et al., 2018; Wang et al., 2001). For example, Pbp2 is the only bifunctional *S. aureus* penicillin-binding protein (transglycosylase and transpeptidase activities) (Goffin and Ghuysen, 1998; Murakami, 1994) and is involved in cell wall cross-linking. Pbp2 has also been associated with susceptibility to membrane and cell-wall targeting antibiotics (Łęski and Tomasz, 2005; Sieradzki and Tomasz, 1999). Besides the shared mutations, there were a number of media-specific mutations (Figure 3B). This environmental dependency was also evident from the expression of these key mutated genes (Figure 3C). For example, *vraG* and *mprF* genes that are mostly mutated in CA-MHB condition were highly expressed in vancomycin-tolerized strains in the same media, while there was no differential expression in RPMI+. On the other hand, some genes that seem to be mutated in a condition-specific manner presented a similar transcriptional profile in both (*e.g., sgtB* and *prsA*). Again, most of the key mutated genes were related to cell wall biosynthesis (e.g., *sgtB, prsA, walK, vraT, pbp2, mprF*). However, there were other key mutated genes associated with transcription (*rpoC*), transport (*pitA_1, vraG*), regulation (*perR, melR_2*), metabolism (*mqo2*), pathogenesis (*ebh_1*) and unknown function (*RS08780*).

bioRxiv preprint doi: https://doi.org/10.1101/2020.06.07.138933; this version posted June 7, 2020. The copyright holder for this preprint (which was not certified by peer review) is the author/funder, who has granted bioRxiv a license to display the preprint in perpetuity. It is made available under aCC-BY 4.0 International license.

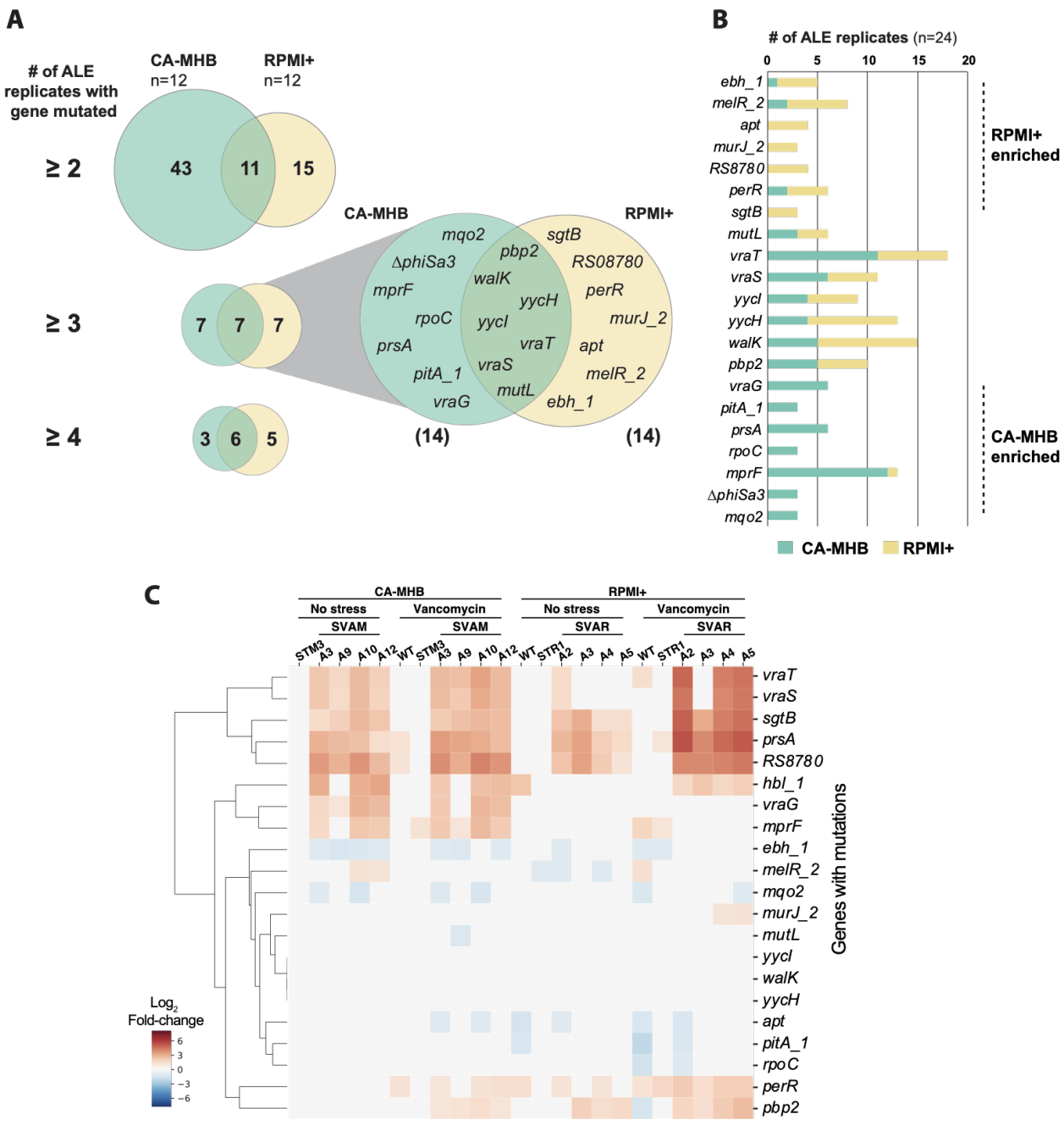

Figure 3. Key mutations found in MRSA during vancomycin tolerization. (A) Venn diagrams of the number of key mutated genes in the two utilized media conditions (i.e., CA-MHB and RPMI+). (B) A bar plot of the number of lineages with mutations in a key mutated gene, n=24 lineages, 12 for each media condition. (C) A heatmap of

bioRxiv preprint doi: https://doi.org/10.1101/2020.06.07.138933; this version posted June 7, 2020. The copyright holder for this preprint (which was not certified by peer review) is the author/funder, who has granted bioRxiv a license to display the preprint in perpetuity. It is made available under aCC-BY 4.0 International license.

252 expression level of key mutated genes in a selection of starting and TALE-derived
253 strains, in the presence and absence of vancomycin. STM: *Staphylococcus aureus*
254 adapted to CA-MHB. STR: *Staphylococcus aureus* adapted to RPMI+. SVAM:
255 *Staphylococcus aureus* tolerized to vancomycin in CA-MHB. SVAR: *Staphylococcus*
256 *aureus* tolerized to vancomycin in RPMI+.
257
258
259 Mutational analysis of TALE clones from CA-MHB revealed an instance of parallel
260 evolution involving excision of the prophage ΦSa3 in three independent lineages. Large
261 identical genomic deletions of 43,048 bp resulted from the excision of prophage ΦSa3,
262 the most prevalent prophage family in *S. aureus (Xia and Wolz, 2014)*, which encodes for
263 the immune evasion cluster (Goerke et al., 2009; Verkaik et al., 2011). This cluster
264 harbors the immune modulators staphylokinase (Sak), staphylococcal complement
265 inhibitor (SCIN), staphylococcal enterotoxin A (Sea), and chemotaxis inhibitory protein of
266 *S. aureus* (CHIPS) (Read et al., 2018; van Wamel et al., 2006; Verkaik et al., 2011).
267 Excision of the prophage results in the repair of the β-hemolysin gene (*hlb*) (Figure 4A)
268 (Tran et al., 2019). Selective excision of prophage ΦSa3 has been reported, suggesting
269 it acts as a molecular regulatory switch for β-hemolysin production (Tran et al., 2019).
270 Testing of hemolytic activity of two of the three TALE strains and their starting strain
271 counterparts confirmed one other characteristic phenotype observed in VISA strains,
272 reduced hemolytic activity (Figure 4B). Since *hlb* encodes for a cold active hemolysin,
273 after 24h incubation at 4 °C, it was possible to observe acquired hemolytic activity for the
274 TALE strains which have excised the prophage ΦSa3 (Figure 4C), strains SVAM_A10

bioRxiv preprint doi: https://doi.org/10.1101/2020.06.07.138933; this version posted June 7, 2020. The copyright holder for this preprint (which was not certified by peer review) is the author/funder, who has granted bioRxiv a license to display the preprint in perpetuity. It is made available under aCC-BY 4.0 International license.

and SVAM_A12. In contrast, none of the RPMI+ media tolerized strains excised the prophage (Figure 3B). The expression of genes encoded in the prophage was analyzed in TALE strains derived from both media environments and it was observed that there was higher transcriptional activity of prophage genes in RPMI+ as compared to CA-MHB, for strains which retained the prophage genes (Figure 4D). This observation suggests an advantage in maintaining these prophage genes in RPMI+ upon vancomycin stress.

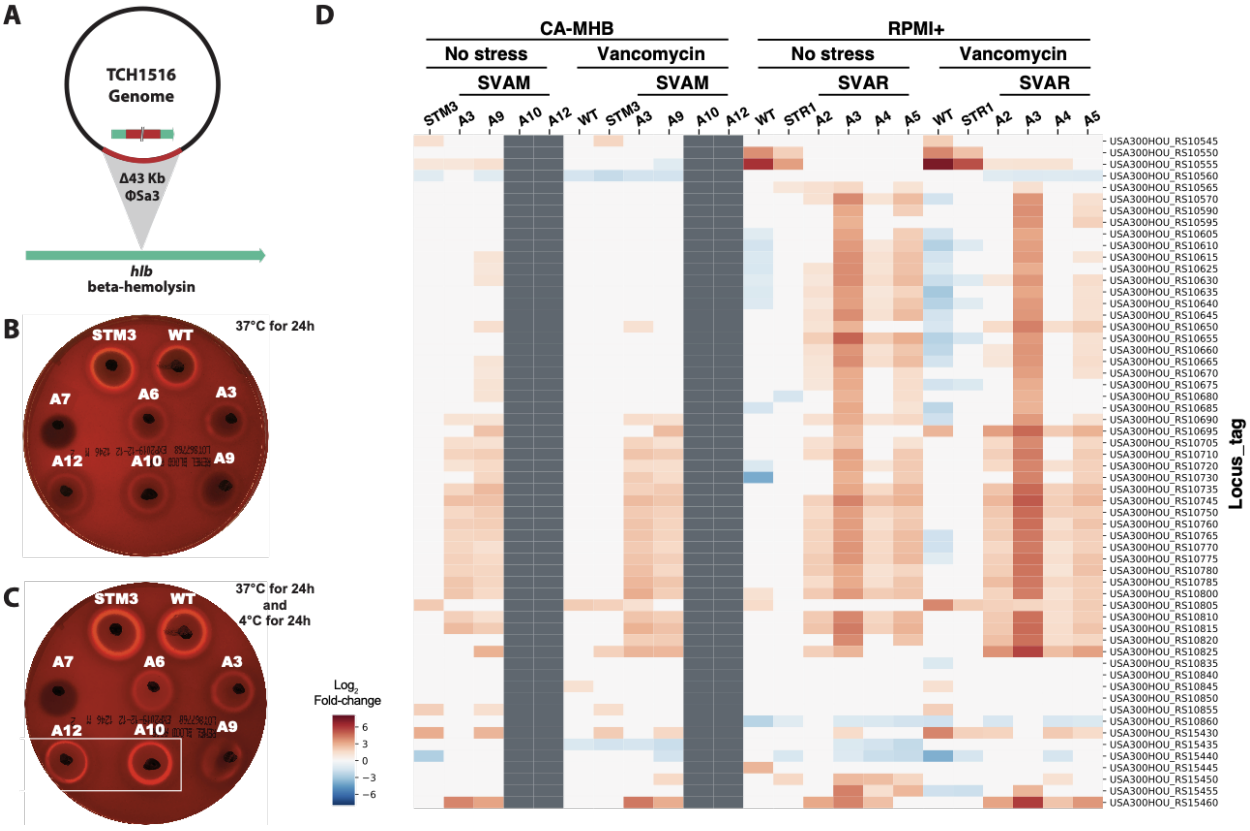

Figure 4. The excision of ΦSa3 prophage. (A) Schematic representation of the excision of the ΦSa3 prophage from the TCH1516 genome which leads to the repair of *hlb* gene, encoding for a β-hemolysin. (B) An image of a plate displaying hemolytic activity after 24 h incubation at 37 °C for vancomycin TALE strains in CA-MHB and their corresponding starting strains, wild-type (WT) TCH1516 and CA-MHB media-adapted STM3. (C) An image of the same plate in B displaying hemolytic activity following an

bioRxiv preprint doi: https://doi.org/10.1101/2020.06.07.138933; this version posted June 7, 2020. The copyright holder for this preprint (which was not certified by peer review) is the author/funder, who has granted bioRxiv a license to display the preprint in perpetuity. It is made available under aCC-BY 4.0 International license.

additional 24 h incubation at 4 °C, to assess cold hemolytic activity of β-hemolysin. Increased hemolytic activity can be seen for strains SVAM_A10 and SVAM_A12 (boxed). (D) A heatmap of expression levels of genes encoded within the prophage ΦSa3. Grey indicates absence of the gene in a strain due to excision of the prophage. STM: *Staphylococcus aureus* adapted to CA-MHB. STR: *Staphylococcus aureus* adapted to RPMI+. SVAM: *Staphylococcus aureus* tolerized to vancomycin in CA-MHB. SVAR: *Staphylococcus aureus* tolerized to vancomycin in RPMI+.

Broad scale impact of mutations in regulatory genes. The most commonly mutated genes in both media conditions during the TALE experiments were annotated with regulatory functions, with the *walRKyycHI* and *vraRST* operons being the most targeted (Figure 3B). Interestingly, the accessory genes (i.e., *yycH*, *yycI* and *vraT*) known to impact the activity of these regulators (Boyle-Vavra et al., 2013; Cameron et al., 2016), were some of the most often mutated. Mutations in regulatory genes tend to impact bacterial responses on a broad scale, which is difficult to assess solely from mutational data. Therefore, we performed RNAseq with and without vancomycin stress to understand how the mutations observed impacted the transcriptional profile of the evolved strains. Within the previously characterized WalR regulon (Delauné et al., 2012), there were several genes differentially regulated in the vancomycin TALE clones. In fact, both upregulation and downregulation was observed in several genes within this regulon (Figure 5A, and Supplementary Figure 3). Downregulation of the *spa* gene and lower hemolytic activity are a characteristic of VISA strains (Howden et al., 2010), which was also confirmed from the acquired transcriptional data (Figure 5A). The pyrimidine operon has been deemed

bioRxiv preprint doi: https://doi.org/10.1101/2020.06.07.138933; this version posted June 7, 2020. The copyright holder for this preprint (which was not certified by peer review) is the author/funder, who has granted bioRxiv a license to display the preprint in perpetuity. It is made available under aCC-BY 4.0 International license.

311 important for growth in RPMI+ (Poudel et al., 2020) and was upregulated in strains
312 evolved in this medium. The VraR regulon, responsible for the control of the cell wall
313 stimulon, showed an overall upregulation in vancomycin-adapted strains (Figure 5B). The
314 most upregulated genes, *vraX* and *cwrA*, are described to be part of both regulons (Figure
315 5), and have both been linked to cell wall stress response (Balibar et al., 2010; F.
316 McAleese et al., 2006). Even though all the characterized vancomycin-tolerized strains
317 presented a similar transcriptional rearrangement of these regulons, the analyzed strains
318 carried distinct mutations in these regulatory genes (35 and 42 total different mutations in
319 the *vra* and *wal* regulons, respectively; Supplementary Tables 3 and 4), suggesting that
320 multiple mutational mechanisms can result in a similar transcriptional landscape. Overall,
321 the TALE-derived mutations in these regulatory systems form a defined set of multiple
322 unique mutations and resulted in significant rearrangements in expression levels of genes
323 strongly associated with the observed tolerance phenotypes.

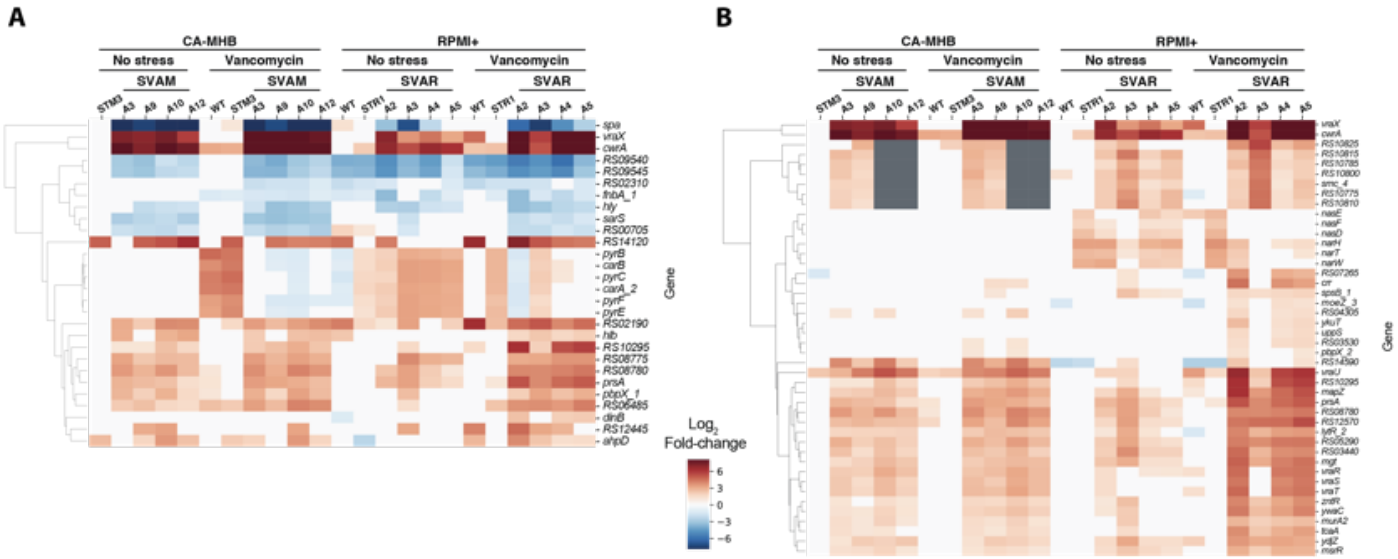

324

325 **Figure 5.** Rearranged transcriptional landscapes of operons associated with
326 vancomycin tolerance in TALE strains. (A) A heatmap of expression levels of the genes

bioRxiv preprint doi: https://doi.org/10.1101/2020.06.07.138933; this version posted June 7, 2020. The copyright holder for this preprint (which was not certified by peer review) is the author/funder, who has granted bioRxiv a license to display the preprint in perpetuity. It is made available under aCC-BY 4.0 International license.

in the WalR regulon (Delauné et al., 2012) displaying significant levels of differential expression, both up and down. (B) Expression of genes in the VraR cell wall stimulon (Boyle-Vavra et al., 2013). STM: *Staphylococcus aureus* adapted to CA-MHB. STR: *Staphylococcus aureus* adapted to RPMI+. SVAM: *Staphylococcus aureus* tolerized to vancomycin in CA-MHB. SVAR: *Staphylococcus aureus* tolerized to vancomycin in RPMI+.

Elucidation of molecular mechanisms in vancomycin tolerance. Multiple mutations in *mprF* were observed in CA-MHB vancomycin-tolerized strains and were validated to display a significant decrease in negative cell surface charge. *mprF* encodes for a multi peptide resistance factor and has been associated with increased resistance to daptomycin and antimicrobial peptides (Ernst et al., 2018; Ernst and Peschel, 2019). Besides the previously described regulatory gene mutations, *mprF* was the most mutated gene in strains tolerized to vancomycin in CA-MHB. In the 12 CA-MHB-tolarized lineages, we identified seven previously reported mutations that lead to resistance through a MprF mechanism, and extended this knowledge base by identifying 10 new mutations (Figure6A). The MprF described resistance mechanism consists of decreasing the negative cell surface charge, and therefore repulsing cationic antimicrobial peptides and daptomycin (Ernst and Peschel, 2019). Since vancomycin is also a positively-charged peptide, one can speculate that this general mechanism would lead to increased vancomycin tolerance. In order to support this, we characterized the cell surface charge in tolerized mutants and its starting strain counterparts (Figure 6B). Tolerized mutants, with amino acid changes towards the C-terminal part of MprF, had a significant decrease

bioRxiv preprint doi: https://doi.org/10.1101/2020.06.07.138933; this version posted June 7, 2020. The copyright holder for this preprint (which was not certified by peer review) is the author/funder, who has granted bioRxiv a license to display the preprint in perpetuity. It is made available under aCC-BY 4.0 International license.

in negative cell surface charge (Figure 6B and 6C). Strain SVAM_A3, with an amino acid change at position 50 (R50C), did not have a significant change in cell surface charge, which explains the observation of mutational hot-spots between positions 278 to 510 (Figure 6A). Thus, a similar mechanism of shifting the cell surface charge from more to less negatively-charged was validated for a subset of the *mprF* mutants uncovered from the TALE experimentation in this study.

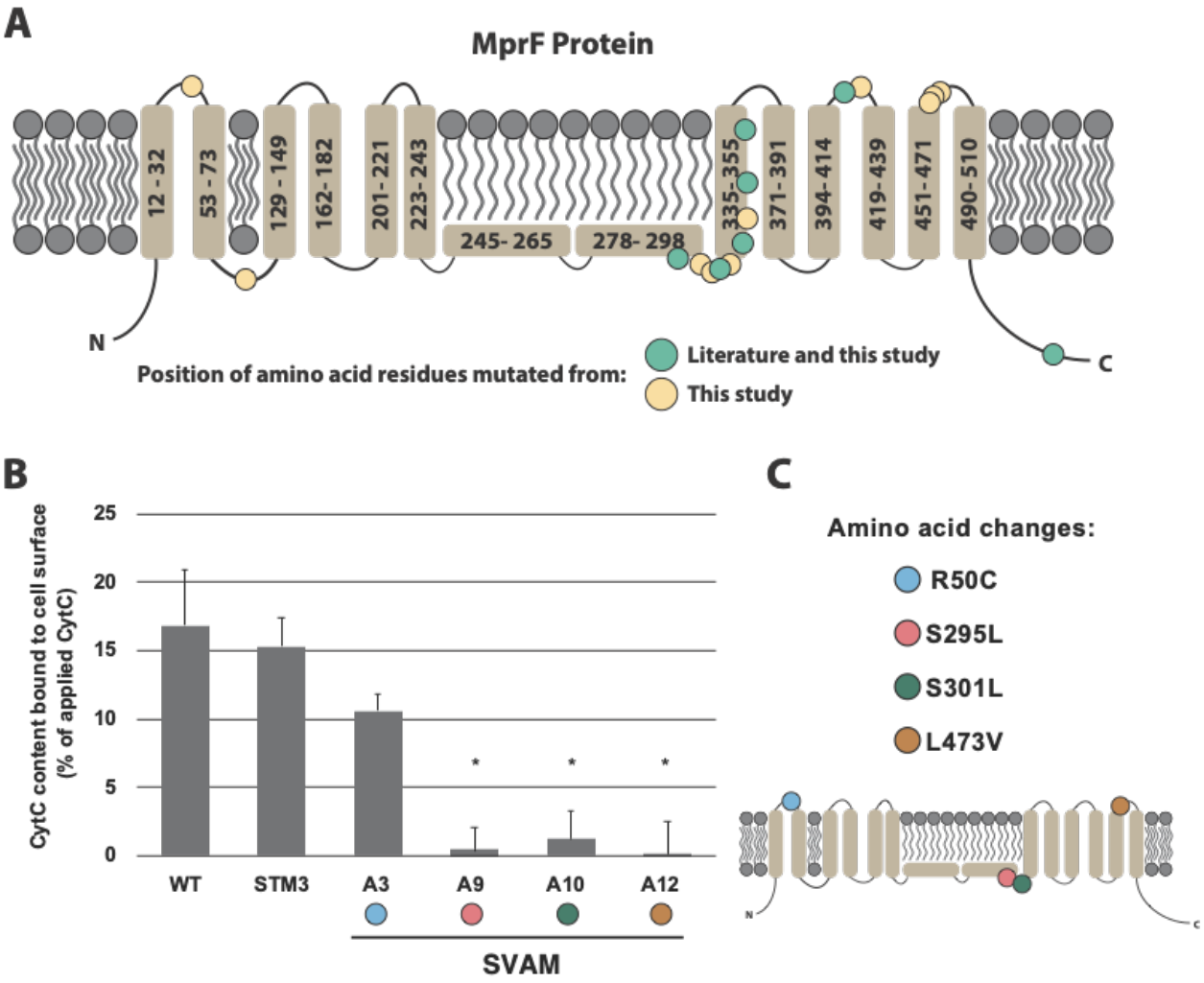

Figure 6. MprF mutations and their effect on cell surface charge. (A) Topology of the MprF membrane protein and mapping of mutations identified in this dataset (yellow and green circles), in comparison to previously reported ones (green circles) (Ernst and

bioRxiv preprint doi: https://doi.org/10.1101/2020.06.07.138933; this version posted June 7, 2020. The copyright holder for this preprint (which was not certified by peer review) is the author/funder, who has granted bioRxiv a license to display the preprint in perpetuity. It is made available under aCC-BY 4.0 International license.

Peschel, 2019). (B) A graph quantifying the cell surface charge of strains tolerized to vancomycin, in comparison to their starting strain counterparts. Values that are significantly different ($P \leq 0.05$) from the value for the respective starting strain (WT or STM3) by Student's t-Test are indicated by an asterisk. (C) Identified locations of the specific amino acid substitutions observed in the tolerized strains and their position in the MprF structure. These mutations correspond to the strains tested in panel B. STM: *Staphylococcus aureus* adapted to CA-MHB. SVAM: *Staphylococcus aureus* tolerized to vancomycin in CA-MHB.

Association of genetic targets with decreased susceptibility. Gene inactivation enables the assessment of a given gene's role in tolerance. In order to understand the importance of the mutated and highly expressed genes in vancomycin tolerance, we relied on the available *S. aureus* Nebraska Transposon Mutant Library (Fey et al., 2013). We identified five genes required for tolerance and five genes impairing tolerance. A selection of mutants in key mutated genes or highly expressed genes was evaluated for their vancomycin susceptibility in both environmental conditions (Table 1). Interestingly, reduced vancomycin susceptibility was seen for all strains when testing was performed in RPMI+ compared to CA-MHB, in some instances with 2-fold or greater increases in vancomycin MIC in RPMI+. Media-specific susceptibility was observed for several mutants, similar to what was observed with the TALE-derived clones. Transposon inactivation of genes *yycI*, *sgtB*, *melR_2*, *stp*, and *lytM_2* resulted in a decreased susceptibility to vancomycin in RPMI+, but no difference in CA-MHB. On the other hand, *vraT*, *vraR*, *vraS*, *vraG* and *mprF* showed an increased susceptibility to vancomycin in

bioRxiv preprint doi: https://doi.org/10.1101/2020.06.07.138933; this version posted June 7, 2020. The copyright holder for this preprint (which was not certified by peer review) is the author/funder, who has granted bioRxiv a license to display the preprint in perpetuity. It is made available under aCC-BY 4.0 International license.

383 CA-MHB, but no difference in RPMI+. The fact that gene inactivation can lead to
384 decreased susceptibility is noteworthy as 57 (15.3%) and 76 (16.5%) of the total
385 mutations identified lead to likely gene disruption in the RPMI+ and CA-MHB datasets,
386 respectively. It is noteworthy that some of the gene disruptions identified in our datasets
387 were in the same genes that showed here a higher MIC upon inactivation, specifically
388 *yycI* and *stp* (in both media conditions), *melR_2* (only in RPMI+), and *lytM_2* (only in CA-
389 MHB) (Supplementary Tables 3 and 4). These findings not only confirm the role of several
390 genes (i.e. *yycI*, *sgtB*, *melR_2*, *stp*, *lytM_2, vraT*, *vraR*, *vraS*, *vraG* and *mprF*) in
391 vancomycin tolerance, but also highlight the different roles these have in the development
392 of resistance under varying environmental conditions.
393
394 **Table 1 -** Minimum inhibitory concentration (MIC_{90}) of *S. aureus* Nebraska Transposon
395 Mutant Library (Fey et al., 2013) in both environmental conditions, CA-MHB and RPMI+.
396 Strain ID refers to the NE identifier and the wild-type strain used in the generation of the
397 transposon mutants (JE2). Gene indicates the gene that has been disrupted by the
398 transposon.

		MIC_{90} (µg/mL)	
Strain ID	**Gene**	**CA-MHB**	**RPMI+**
JE2	-	1	2
NE1693	*yycH*	1	2
NE1865	*yycI*	1	4

bioRxiv preprint doi: https://doi.org/10.1101/2020.06.07.138933; this version posted June 7, 2020. The copyright holder for this preprint (which was not certified by peer review) is the author/funder, who has granted bioRxiv a license to display the preprint in perpetuity. It is made available under aCC-BY 4.0 International license.

NE596	*sgtB*	1	4
NE1304	*melR_2*	1	4
NE1919	*stp*	1	4
NE641	*lytM_2*	1	4
NE274	*vraT*	0.5	2
NE554	*vraR*	0.5	1 - 2
NE823	*vraS*	0.5	2
NE70	*vraG*	0.25 - 0.5	2
NE1360	*mprF*	0.25 - 0.5	2
NE665	*perR*	0.5 - 1	2
NE387	*cwrA*	1	2

399

bioRxiv preprint doi: https://doi.org/10.1101/2020.06.07.138933; this version posted June 7, 2020. The copyright holder for this preprint (which was not certified by peer review) is the author/funder, who has granted bioRxiv a license to display the preprint in perpetuity. It is made available under aCC-BY 4.0 International license.

Discussion

The expanding problem of antibiotic resistant pathogens has been discussed for almost a century (Podolsky, 2018), but we remain in the infancy of understanding its complexity. In this study, we sought to understand changes in susceptibility, mutational mechanisms which enable such chances, and phenotypic responses of tolerant strains by analyzing growth screens, transcriptomics, and specific assays for evolved and mutated strains of MRSA under multiple media conditions. The main findings from this work are that (i) TALE successfully generated tolerant strains in both media types, although tolerance phenotypes translated across media types for CA-MHB TALE-derived strains, the inverse was not true for RPMI+; (ii) analysis of key mutational mechanisms revealed that numerous genetic allele variations can lead to similar transcriptional and phenotypic changes, especially in the CA-MHB condition; and (iii) TALE-derived strains shared similar properties to resistant clinical isolates in phenotype, mutation types, and gene expression.

There were a number of specific findings that provide context for the main conclusions of this study. These include, (i) the majority of TALE-derived strains tested maintained a tolerant phenotype after prolonged evolution under a no vancomycin stress condition; (ii) greater heterogeneity was found in the mutations observed in TALE-derived strains to become tolerant in CA-MHB than RPMI+, with a set of shared mutational mechanisms on the gene level from TALE-derived strains under both media conditions (enriched in cell wall related regulators), which resulted in major changes in expression for the operons they regulate even though the unique alleles differed; (iii) mutations in *mprF* are a key mechanism in CA-MHB, which decreased the overall negative cell surface charge and

bioRxiv preprint doi: https://doi.org/10.1101/2020.06.07.138933; this version posted June 7, 2020. The copyright holder for this preprint (which was not certified by peer review) is the author/funder, who has granted bioRxiv a license to display the preprint in perpetuity. It is made available under aCC-BY 4.0 International license.

supposedly limited vancomycin access to the cell wall; (iv) similarly to clinically isolated strains, TALE-derived strains had lower hemolytic activity and reduced autolysis (Howden et al., 2010), mutations of the nature of pseudogenization (Mwangi et al., 2007), and similar transcriptional changes for virulence associated genes (e.g., *spa* (Howden et al., 2008; Fionnuala McAleese et al., 2006), *agr* (Mwangi et al., 2007; Sakoulas et al., 2002)); and lastly, (v) different genetic targets have enhancing or impairing roles in tolerance, depending on the environmental condition. Taken together, these findings provide specific information for a change in susceptibility for an important pathogen, an antibiotic commonly used to treat it, and media conditions relevant for human host infection and antimicrobial testing. Moreover, they provide context for the overall development of antibiotic resistance under multiple conditions and independent lineages that can be used to understand the issue as a whole.

The environmental conditions analyzed here were intended to represent both the *in vivo* environment simulating the condition of human infection, and the environment under which standard antimicrobial susceptibility is performed in the clinical laboratory. We showed that the evolutionary strategies adopted in each condition overlap on two major regulatory systems, VraR and WalR, which are responsible for the homeostasis of cell wall (Boyle-Vavra et al., 2013; Dubrac et al., 2007; McCallum et al., 2011; Villanueva et al., 2018) and had been previously linked to glycopeptide resistance (Howden et al., 2010; Hu et al., 2016; Kato et al., 2010). More interesting is the fact that besides such regulatory mutations, which seem to confer similar transcriptional rearrangements, other mutations were largely media-dependent, suggesting that the different media utilized restricted the evolutionary process differently. We have previously shown that growth of *S. aureus* in

bioRxiv preprint doi: https://doi.org/10.1101/2020.06.07.138933; this version posted June 7, 2020. The copyright holder for this preprint (which was not certified by peer review) is the author/funder, who has granted bioRxiv a license to display the preprint in perpetuity. It is made available under aCC-BY 4.0 International license.

RPMI+ and CA-MHB lead to large transcriptional landscape changes (Poudel et al., 2020). In RPMI+, the buffering system used is bicarbonate, a ubiquitous buffer found in humans, which has been shown to potentiate the activity of several antibiotics by dissipating the proton motive force in bacteria (Ersoy et al., 2017; Farha et al., 2018; Kumaraswamy et al., 2016). This process might be one of the major reasons for the distinct evolutionary strategies observed under different media. For instance, this is likely the reason why we do not observe *mprF* mutations in the RPMI+ evolved strains, but we do in all the CA-MHB TALE lineages. MprF activity leads to the alteration of the cell surface charge (Ernst et al., 2018; Ernst and Peschel, 2019), but in the case of RPMI+ the membrane proton motive force is already compromised by the bicarbonate buffer system (Farha et al., 2018), making it an evolutionarily less viable solution towards vancomycin tolerance in this media. The tolerance mechanism through *mprF* mutation also explains the extended lag phase observed for all the strains tolerized in CA-MHB media, since an altered cell surface charge impacts bacterial cell division (Li et al., 2016; Strahl and Hamoen, 2010).

Even though both media used in vancomycin tolerizations resulted in highly tolerant vancomycin strains, in the case of strains evolved in RPMI+, this phenotype did not translate to CA-MHB media. Media dependent susceptibilities have been previously reported (Ersoy et al., 2017; Farha et al., 2018; Kumaraswamy et al., 2016; Lin et al., 2015). Here we showed that the evolution of resistance in physiological conditions is not phenotypically revealed in clinical susceptibility testing (Figure 2B). The fact that decreased vancomycin susceptibility acquired in RPMI+ simulates the selective conditions under which it evolves in patients receiving vancomycin (McKee and

bioRxiv preprint doi: https://doi.org/10.1101/2020.06.07.138933; this version posted June 7, 2020. The copyright holder for this preprint (which was not certified by peer review) is the author/funder, who has granted bioRxiv a license to display the preprint in perpetuity. It is made available under aCC-BY 4.0 International license.

Komarova, 2017), and that these changes are not detected in the CA-MHB utilized laboratory testing essentially shows that the clinical laboratory is blind to the clinically relevant reduction in vancomycin susceptibility that evolves in *S. aureus*. This may explain the poor clinical efficacy of vancomycin even against *S. aureus* isolates that the laboratory designates as susceptible. Clinical experience is abundant with patients with MRSA bacteremia by organisms fully susceptible to vancomycin, yet fail to clear their infection despite adequate dosing and the lack of surgical solutions. The clinical laboratory shortcomings in detecting vancomycin resistance in *S. aureus* may be one explanation for the fact that vancomycin is unique among anti-staphylococcal antibiotics where resistance took decades to emerge (at least according to the laboratory). Resistance to every anti-staphylococcal antibiotic has emerged just a few years after the clinical introduction of that antibiotic, yet for vancomycin, which was introduced into clinical practice in 1958, VISA was not described until 1997 (Levine, 2006). Examining these data at an even higher level shows that every mutant from the Nebraska library demonstrated a higher vancomycin MIC in RPMI+ compared to CA-MHB. Given that the area under the curve (AUC)/MIC ratio is the pharmacokinetic target reflective of vancomycin activity suggests considerably weaker activity of vancomycin *in vivo* than in clinical laboratory conditions would indicate (Giuliano et al., 2010). Indeed, the well-described clinical-microbiological discordance of vancomycin with regards to *S. aureus* explained by our findings supports serious re-examination of how antimicrobial susceptibility paradigms can be made more clinically relevant (Ersoy et al., 2017).

During the many years that antibiotic resistance has been studied, associations have been made between specific alleles and decreased antibiotic susceptibility (Cameron et

bioRxiv preprint doi: https://doi.org/10.1101/2020.06.07.138933; this version posted June 7, 2020. The copyright holder for this preprint (which was not certified by peer review) is the author/funder, who has granted bioRxiv a license to display the preprint in perpetuity. It is made available under aCC-BY 4.0 International license.

al., 2012; Howden et al., 2011, 2010; Hu et al., 2015, 2016; Ishii et al., 2015; Mwangi et al., 2007; Vidaillac et al., 2013). Numerous surveys have been conducted using PCR and sequencing to determine the likelihood of a given strain to be less susceptible to a given antibiotic (Costa et al., 2018; Kato et al., 2010; Sabat et al., 2018; Shore et al., 2010). Here we showed that limiting the analysis to a handful of genes can be misleading and that many allele variants can result in the same outcome. We identified several mutations in alleles previously associated with decreased susceptibility, with most of the mutations being new variants. A high-throughput approach utilizing ALE was an efficient way to sample the evolutionary pathways available for the development of antibiotic resistance, while expanding on the knowledge of allelic variation responsible for such phenotypes. Examples provided here are the mutations in the regulatory systems (i.e., *vraSRT* and *walKRyycHI*) and in *mprF*. We showed that different allele variants in regulatory genes can impact the transcriptional landscape similarly. We have largely expanded the knowledge on *mprF* allele variants that result in altered cell surface charge that might lead to decreased vancomycin susceptibility and bridge the knowledge gap between vancomycin and peptide antibiotic cross-resistance.

Pseudogenization is another type of genetic variance we believe merits attention. We previously showed that *S. aureus* restored pseudogenes in order to overcome metabolic limitations (Machado et al., 2019). In this dataset, approximately 15% of all the mutations led to pseudogenization, which can translate into decreased susceptibility, as demonstrated with the transposon mutants (Table 1). This strengthens the hypothesis that *S. aureus* can use this pseudogenization mechanism to adapt to distinct environments, including the development of antibiotic resistance. A study looking at the

bioRxiv preprint doi: https://doi.org/10.1101/2020.06.07.138933; this version posted June 7, 2020. The copyright holder for this preprint (which was not certified by peer review) is the author/funder, who has granted bioRxiv a license to display the preprint in perpetuity. It is made available under aCC-BY 4.0 International license.

adaptive evolution of *S. aureus* during chronic endobronchial infection of a cystic fibrosis patient during 26 months identified 391 mutations (comparable to our datasets) with none of the mutations predicted to result in pseudogene formation (McAdam et al., 2011). The rates at which pseudogenization occurs and reverts, requires further experimental evidence in order to support this method as a common evolutionary strategy in *S. aureus*.

In conclusion, the application of ALE to develop *S. aureus* strains tolerized to vancomycin was successful and links can be drawn between TALE-derived strains and clinical isolates. Susceptibility was not only decreased for the targeted antibiotic, but also reproduced phenotypes similar to the ones previously reported for clinical strains with decreased vancomycin susceptibility (Howden et al., 2010). Furthermore, it allowed us to understand evolutionary strategies and constraints in two clinically relevant media environments while expanding our knowledge on the diversity of alleles contributing to the vancomycin tolerant phenotype. These findings allow a better understanding of the evolution of antibiotic resistance and provide new information valuable for the epidemiological surveillance and control of *S. aureus* resistance in clinical environments. Most importantly, these data call into question the clinical reliability of *S. aureus* vancomycin susceptibility testing as it is currently performed in the clinical laboratory by providing a deeper understanding of why *S. aureus* resistance to vancomycin is rare in the laboratory yet vancomycin treatment failure is common in clinical practice.

bioRxiv preprint doi: https://doi.org/10.1101/2020.06.07.138933; this version posted June 7, 2020. The copyright holder for this preprint (which was not certified by peer review) is the author/funder, who has granted bioRxiv a license to display the preprint in perpetuity. It is made available under aCC-BY 4.0 International license.

Material and Methods

Tolerization Adaptive Laboratory Evolution (TALE)

TALE was performed as previously described (Mohamed et al., 2017), with variations as noted. Four replicates of each starting strain (wild type and two media-adapted strains per media type) were inoculated from independent colonies on LB-agar plates. Cultures were grown in 15 ml working volume tubes which were heated to 37°C and were aerobically stirred at 1100 rpm. Periodically, optical density readings at a 600 nanometer wavelength (OD_{600}) were taken for each culture with a Tecan Sunrise reader plate, until the OD_{600} reached approximately 0.6 (approximately equivalent to an OD_{600} of 1 on a cm path length reader). At that time, 150 µl of the culture was passed to a fresh tube, to prevent the cells from reaching stationary phase. The passage volume was adjusted dynamically based on the actual OD_{600} at the time of passage, to keep the number of cells passed consistent. Additionally, if the culture had grown for several consecutive flasks (~3 flasks), the vancomycin concentration in the next tube was increased. This stepwise increase began at 20% of the starting concentration but augmented over the course of the experiment. Growth rates were estimated for each tube by linear regression of the natural log of the optical density vs. time. Periodically throughout the experiment, culture aliquots were taken for long term storage at -80°C by mixing 800 µL of 50% glycerol with 800 µL of culture.

Whole genome re-sequencing

DNA sequencing was performed on clones and populations throughout the evolution, covering two or three timepoints of the evolution. Total genomic DNA was sampled from

bioRxiv preprint doi: https://doi.org/10.1101/2020.06.07.138933; this version posted June 7, 2020. The copyright holder for this preprint (which was not certified by peer review) is the author/funder, who has granted bioRxiv a license to display the preprint in perpetuity. It is made available under aCC-BY 4.0 International license.

an overnight culture and extracted using a KingFisher Flex Purification system previously validated for the high throughput platform mentioned below (Marotz et al., 2017). Sequencing libraries were prepared using a miniaturized version of the Kapa HyperPlus Illumina-compatible library prep kit (Kapa Biosystems). DNA extracts were normalized to 5 ng total input per sample using an Echo 550 acoustic liquid handling robot (Labcyte Inc), and 1/10 scale enzymatic fragmentation, end-repair, and adapter-ligation reactions carried out using a Mosquito HTS liquid-handling robot (TTP Labtech Inc). Sequencing adapters were based on the iTru protocol (Glenn et al., 2019) , in which short universal adapter stubs are ligated first and then sample-specific barcoded sequences added in a subsequent PCR step. Amplified and barcoded libraries were then quantified using a PicoGreen assay and pooled in approximately equimolar ratios before being sequenced on an Illumina HiSeq 4000 instrument.

The obtained sequencing reads were trimmed and filtered using AfterQC software, version 0.9.6 (Chen et al., 2017). Re-sequencing analysis for mutation identification was performed using the breseq bioinformatics pipeline (Deatherage and Barrick, 2014), version 0.31.1 and the *S. aureus* TCH1516 reference genome (GCA_000017085.1), reannotated using PATRIC (Brettin et al., 2015). ALEdb was used for mutation analysis (Phaneuf et al., 2018).

Minimum inhibitory concentration

Strains were pre-cultured in the corresponding media (CA-MHB or RPMI+10%LB) for ~5h, and then inoculated to a final OD of 0.002 in media with or without vancomycin (Sigma). Growth was measured by following OD_{600} in a Bioscreen C Reader system with

bioRxiv preprint doi: https://doi.org/10.1101/2020.06.07.138933; this version posted June 7, 2020. The copyright holder for this preprint (which was not certified by peer review) is the author/funder, who has granted bioRxiv a license to display the preprint in perpetuity. It is made available under aCC-BY 4.0 International license.

150 µL per well. MIC_{90} was determined at 17 h post incubation. The experiments were done in biological triplicates.

Estimation of growth parameters

Growth parameters were estimated as previously described (Anand et al., 2020). Briefly, lag phase was estimated by fitting the Baranyi growth model (Baranyi and Roberts, 1994) using nonlinear regression in R. A sensitivity analysis was run to exclude data points beyond a specific time threshold T, to avoid skewing the estimated parameters as a result of a possible cell death phase, secondary growth phase or noise. The sensitivity analysis ensured that the lag phase, exponential phase and stationary phase only are taken into account in the fitting process, because all other growth/death phases are not explicitly modeled in Baranyi's equation. Anova was run in R using aov() to test the null hypothesis that there is no difference in lag phase duration between pre-evolved strains (WT, STM2, STM3, STR1 and STR4) and vancomycin adapted strains.

Resistance phenotype stability

Following TALE adaptation to vancomycin, a subset of the TALE strains (6 from each media) were further evolved in duplicate in the respective media for 21.79 ± 2.08 passages, $9.41 \times 10^{11} \pm 9.84 \times 10^{10}$ CCDs. The final populations were then evaluated for their vancomycin susceptibility as described above.

Transcriptomics

bioRxiv preprint doi: https://doi.org/10.1101/2020.06.07.138933; this version posted June 7, 2020. The copyright holder for this preprint (which was not certified by peer review) is the author/funder, who has granted bioRxiv a license to display the preprint in perpetuity. It is made available under aCC-BY 4.0 International license.

Eight TALE strains were selected for transcriptional analysis, along with their pre-evolved counterparts (wild type and one media-adapted strain per medium). Total RNA was sampled from biological duplicate cultures. The strains were grown in each respective media, with and without vancomycin (at 1/2 MIC). At OD 0.2, cultures without vancomycin were harvested. At the same OD, cultures were treated with 0.5x MIC of vancomycin, and harvested for RNA 30min after. Harvesting of the cells consisted in mixing of 3 mL of culture with two volumes of Qiagen RNA-protect Bacteria Reagent (6 ml), vortexed for 5 s, incubated at room temperature for 5 min and immediately centrifuged for 10 min at 17,500 r.p.m.. The supernatant was decanted, and the cell pellet was stored at −80 °C. Total RNA was isolated using the Quick RNA Fungal/Bacterial Microprep (Zymo Research), following vendor procedures, including an on-column DNase treatment. RNA quality and purity was assessed using Nanodrop and Bioanalyzer RNA nano chip. Ribosomal RNA was removed from total RNA preparations using RNaseH. Then secondary structures in the ribosomal RNA were removed by heating to 90 degrees for 1 second, a set of 32-mer DNA oligo probes complementary to the 5S, 16S, and 23S subunits and spaced 9 bases apart were then annealed at 65 degrees followed by digestion with Hybridase (Lucigen), a thermostable RNAseH. The enzyme was added at 65 °C, the reaction incubated for 20 minutes at that temperature, then heated again to 90 °C for 1 second to remove remaining secondary structures, and returned to 65 °C for 10 minutes. The reaction was quickly quenched by the addition of guanidine thiocyanate while still at 65 °C before purifying the mRNA with a Zymo Research RNA Clean and Concentrator kit using their 200 nt cutoff protocol. Carryover oligos were removed with a DNAse I digestion which started at room temperature and gradually increased to 42 °C

bioRxiv preprint doi: https://doi.org/10.1101/2020.06.07.138933; this version posted June 7, 2020. The copyright holder for this preprint (which was not certified by peer review) is the author/funder, who has granted bioRxiv a license to display the preprint in perpetuity. It is made available under aCC-BY 4.0 International license.

over a half hour. This was followed up with another column purification as stated above. The remaining RNA was used to build a cDNA library for sequencing using a KAPA Stranded RNA-seq Library Preparation Kit. The generated cDNA libraries were sent for Illumina sequencing on a HiSeq 4000.

The phred quality scores for the Illumina sequencing reads were generated using FastQC package (Andrews and Others, 2010). Bowtie2 was used to align the raw reads to TCH1516 genome (GCA_000017085.1) and to calculate alignment percentage (Langmead and Salzberg, 2012). The aligned reads were then normalized to transcripts per million (TPM) with DESeq2 (Love et al., 2014). The final expression values were log-transformed $\log_2$[TPM + 1] for visualization and analysis.

Hemolysin production

Analysis of hemolysin production was performed by spotting 10 µL of a OD_{600} culture of 1 grown in CA-MHB onto 5% sheep blood agar plates. Plates were incubated at 37 °C for 24 h, followed by a 4 °C incubation for another 24 h. Hemolysin production was monitored after both incubations by observing the appearance of a clear halo.

Surface charge

Quantification of the relative cell surface charge was performed using a cytochrome C (Sigma) binding assay, as previously described (Peschel et al., 1999). Briefly, cells were grown in CA-MHB until an OD_{600} of ~2, washed twice with MOPS buffer (20 mM, pH 7) and finally resuspended to an OD_{600} of 5. These were incubated for 10 min with 0.5 mg/ml (cytochrome c), which was subsequently removed by centrifugation. The amount of

bioRxiv preprint doi: https://doi.org/10.1101/2020.06.07.138933; this version posted June 7, 2020. The copyright holder for this preprint (which was not certified by peer review) is the author/funder, who has granted bioRxiv a license to display the preprint in perpetuity. It is made available under aCC-BY 4.0 International license.

649 cytochrome C was spectrophotometrically quantified at 530nm. The amount of
650 cytochrome C bound to the cells can be used as a proxy for the cell surface charge. The
651 experiments were done in biological triplicates.

652

653 *Autolysis assay*

654 Evaluation of autolysis was performed using the Triton X-100-induced autolysis assay.
655 Cells were grown to an OD_{600} of 1, washed twice with PBS buffer and resuspended in
656 PBS buffer containing 0.05 % Triton X-100. Cell suspensions were incubated at 37 °C
657 and autolytic activity was measured by monitoring the OD_{600} every hour using Tecan
658 Infinite 200 Pro microplate reader. The experiments were done in biological triplicates.

659

660 *Accession number(s)*

661 Newly determined DNA sequence data were deposited in the NCBI database under
662 BioProject PRJNA521551, accession numbers SRR8552163 to SRR8552250. All RNA-
663 seq data have been deposited to the GEO database (record GSE149213) and Short Read
664 Archive (SRA), RNA-seq data accession numbers SRX8164260 to SRX8164307.

665

666 **Acknowledgements**

667 This research was supported by NIH NIAID grant (U01-AI124316).

bioRxiv preprint doi: https://doi.org/10.1101/2020.06.07.138933; this version posted June 7, 2020. The copyright holder for this preprint (which was not certified by peer review) is the author/funder, who has granted bioRxiv a license to display the preprint in perpetuity. It is made available under aCC-BY 4.0 International license.

Supplemental material

Table S1 - Minimum inhibitory concentration (MIC_{90}) of *S. aureus* starting strains and TALE-derived strains in the same environmental conditions used for tolerance evolution, CA-MHB or RPMI+. Post-TALE refers to the $MIC_{90}$of the population after 21.79 ± 2.08 passages ($9.41x10^{11}$ ± $9.84x10^{10}$ CCDs) in the media used for evolution, without vancomycin. The post-TALE evolution was performed in duplicate for each of the end-point clones.

Figure S1 – Characteristics of vancomycin TALE strains. (A) An image of a plate displaying hemolytic activity after 24 h incubation at 37 °C for starting strains and vancomycin TALE strains (B) Autolysis of whole cells of *S. aureus*. Mid-exponential-phase cultures were resuspended in 0.05 M Tris-HCl (pH 7.2) containing 0.05% Triton X-100 and were incubated at 30°C. Absorbance was measured every hour and percentage to initial absorbance calculated.

Table S2 – ANOVA statistical analysis of the lag-phase duration of starting strains and evolved strains in the same media as that used for tolerization.

Figure S2 – Venn diagram of the key mutated genes (≥ 2 instances) in the two utilized media conditions (i.e., CA-MHB and RPMI+).

bioRxiv preprint doi: https://doi.org/10.1101/2020.06.07.138933; this version posted June 7, 2020. The copyright holder for this preprint (which was not certified by peer review) is the author/funder, who has granted bioRxiv a license to display the preprint in perpetuity. It is made available under aCC-BY 4.0 International license.

689 **Table S3 -** Mutations identified for TALE-derived strains after tolerization to vancomycin
690 in CA-MHB. Nomenclature example A1 F29 I1 R1 = ALE 1 Flask 29 Isolate (I1=clone,
691 I0=population) Replicate 1.
692
693 **Table S4 -** Mutations identified for TALE-derived strains after tolerization to vancomycin
694 in RPMI+. Nomenclature example A1 F29 I1 R1 = ALE 1 Flask 29 Isolate (I1=clone,
695 I0=population) Replicate 1.

bioRxiv preprint doi: https://doi.org/10.1101/2020.06.07.138933; this version posted June 7, 2020. The copyright holder for this preprint (which was not certified by peer review) is the author/funder, who has granted bioRxiv a license to display the preprint in perpetuity. It is made available under aCC-BY 4.0 International license.

References

Alcock BP, Raphenya AR, Lau TTY, Tsang KK, Bouchard M, Edalatmand A, Huynh W, Nguyen A-LV, Cheng AA, Liu S, Min SY, Miroshnichenko A, Tran H-K, Werfalli RE, Nasir JA, Oloni M, Speicher DJ, Florescu A, Singh B, Faltyn M, Hernandez-Koutoucheva A, Sharma AN, Bordeleau E, Pawlowski AC, Zubyk HL, Dooley D, Griffiths E, Maguire F, Winsor GL, Beiko RG, Brinkman FSL, Hsiao WWL, Domselaar GV, McArthur AG. 2020. CARD 2020: antibiotic resistome surveillance with the comprehensive antibiotic resistance database. *Nucleic Acids Res* **48**:D517–D525.

Anand A, Chen K, Catoiu E, Sastry AV, Olson CA, Sandberg TE, Seif Y, Xu S, Szubin R, Yang L, Feist AM, Palsson BO. 2020. OxyR Is a Convergent Target for Mutations Acquired during Adaptation to Oxidative Stress-Prone Metabolic States. *Mol Biol Evol* **37**:660–667.

Andrews S, Others. 2010. FastQC: a quality control tool for high throughput sequence data.

Balibar CJ, Shen X, McGuire D, Yu D, McKenney D, Tao J. 2010. cwrA, a gene that specifically responds to cell wall damage in *Staphylococcus aureus*. *Microbiology* **156**:1372–1383.

Ban C, Yang W. 1998. Crystal structure and ATPase activity of MutL: implications for DNA repair and mutagenesis. *Cell* **95**:541–552.

Baranyi J, Roberts TA. 1994. A dynamic approach to predicting bacterial growth in food. *Int J Food Microbiol* **23**:277–294.

Boyle-Vavra S, Yin S, Jo DS, Montgomery CP, Daum RS. 2013. VraT/YvqF is required

bioRxiv preprint doi: https://doi.org/10.1101/2020.06.07.138933; this version posted June 7, 2020. The copyright holder for this preprint (which was not certified by peer review) is the author/funder, who has granted bioRxiv a license to display the preprint in perpetuity. It is made available under aCC-BY 4.0 International license.

719 for methicillin resistance and activation of the VraSR regulon in *Staphylococcus*
720 *aureus*. *Antimicrob Agents Chemother* **57**:83–95.
721 Brettin T, Davis JJ, Disz T, Edwards RA, Gerdes S, Olsen GJ, Olson R, Overbeek R,
722 Parrello B, Pusch GD, Shukla M, Thomason JA 3rd, Stevens R, Vonstein V,
723 Wattam AR, Xia F. 2015. RASTtk: a modular and extensible implementation of the
724 RAST algorithm for building custom annotation pipelines and annotating batches of
725 genomes. *Sci Rep* **5**:8365.
726 Cameron DR, Jiang JH, Kostoulias X, Foxwell DJ, Peleg AY. 2016. Vancomycin
727 susceptibility in methicillin-resistant *Staphylococcus aureus* is mediated by YycHI
728 activation of the WalRK essential two-component regulatory system. *Sci Rep* **6**:1–
729 11.
730 Cameron DR, Ward DV, Kostoulias X, Howden BP, Moellering RC Jr, Eliopoulos GM,
731 Peleg AY. 2012. Serine/threonine phosphatase Stp1 contributes to reduced
732 susceptibility to vancomycin and virulence in *Staphylococcus aureus*. *J Infect Dis*
733 **205**:1677–1687.
734 Chen S, Huang T, Zhou Y, Han Y, Xu M, Gu J. 2017. AfterQC: automatic filtering,
735 trimming, error removing and quality control for fastq data. *BMC Bioinformatics*
736 **18**:80.
737 Costa SS, Sobkowiak B, Parreira R, Edgeworth JD, Viveiros M, Clark TG, Couto I.
738 2018. Genetic Diversity of norA, Coding for a Main Efflux Pump of *Staphylococcus*
739 *aureus*. *Front Genet* **9**:710.
740 Deatherage DE, Barrick JE. 2014. Identification of mutations in laboratory-evolved
741 microbes from next-generation sequencing data using breseq. *Methods Mol Biol*

bioRxiv preprint doi: https://doi.org/10.1101/2020.06.07.138933; this version posted June 7, 2020. The copyright holder for this preprint (which was not certified by peer review) is the author/funder, who has granted bioRxiv a license to display the preprint in perpetuity. It is made available under aCC-BY 4.0 International license.

1151:165–188.

Delauné A, Dubrac S, Blanchet C, Poupel O, Mäder U, Hiron A, Leduc A, Fitting C, Nicolas P, Cavaillon J-M, Adib-Conquy M, Msadek T. 2012. The WalKR system controls major staphylococcal virulence genes and is involved in triggering the host inflammatory response. *Infect Immun* **80**:3438–3453.

Dragosits M, Mattanovich D. 2013. Adaptive laboratory evolution - principles and applications for biotechnology. *Microb Cell Fact* **12**:1.

Dubrac S, Boneca IG, Poupel O, Msadek T. 2007. New insights into the WalK/WalR (YycG/YycF) essential signal transduction pathway reveal a major role in controlling cell wall metabolism and biofilm formation in Staphylococcus aureus. *J Bacteriol* **189**:8257–8269.

Ernst CM, Peschel A. 2019. MprF-mediated daptomycin resistance. *Int J Med Microbiol*. doi:10.1016/j.ijmm.2019.05.010

Ernst CM, Slavetinsky CJ, Kuhn S, Hauser JN, Nega M, Mishra NN, Gekeler C, Bayer AS, Peschel A. 2018. Gain-of-Function Mutations in the Phospholipid Flippase MprF Confer Specific Daptomycin Resistance. *mBio*. doi:10.1128/mbio.01659-18

Ersoy SC, Heithoff DM, Barnes L 5th, Tripp GK, House JK, Marth JD, Smith JW, Mahan MJ. 2017. Correcting a Fundamental Flaw in the Paradigm for Antimicrobial Susceptibility Testing. *EBioMedicine* **20**:173–181.

Farha MA, French S, Stokes JM, Brown ED. 2018. Bicarbonate Alters Bacterial Susceptibility to Antibiotics by Targeting the Proton Motive Force. *ACS Infect Dis* **4**:382–390.

Fey PD, Endres JL, Yajjala VK, Widhelm TJ, Boissy RJ, Bose JL, Bayles KW. 2013. A

bioRxiv preprint doi: https://doi.org/10.1101/2020.06.07.138933; this version posted June 7, 2020. The copyright holder for this preprint (which was not certified by peer review) is the author/funder, who has granted bioRxiv a license to display the preprint in perpetuity. It is made available under aCC-BY 4.0 International license.

765 genetic resource for rapid and comprehensive phenotype screening of nonessential
766 *Staphylococcus aureus* genes. *MBio* **4**:e00537–12.
767 Gardete S, Kim C, Hartmann BM, Mwangi M, Roux CM, Dunman PM, Chambers HF,
768 Tomasz A. 2012. Genetic pathway in acquisition and loss of vancomycin resistance
769 in a methicillin resistant *Staphylococcus aureus* (MRSA) strain of clonal type
770 USA300. *PLoS Pathog* **8**.
771 Giuliano C, Haase KK, Hall R. 2010. Use of vancomycin pharmacokinetic–
772 pharmacodynamic properties in the treatment of MRSA infections. *Expert Rev Anti*
773 *Infect Ther* **8**:95–106.
774 Glenn TC, Nilsen RA, Kieran TJ, Sanders JG, Bayona-Vásquez NJ, Finger JW, Pierson
775 TW, Bentley KE, Hoffberg SL, Louha S, Garcia-De Leon FJ, del Rio Portilla MA,
776 Reed KD, Anderson JL, Meece JK, Aggrey SE, Rekaya R, Alabady M, Belanger M,
777 Winker K, Faircloth BC. 2019. Adapterama I: universal stubs and primers for 384
778 unique dual-indexed or 147,456 combinatorially-indexed Illumina libraries (iTru &
779 iNext). *PeerJ*. doi:10.7717/peerj.7755
780 Glickman BW, Radman M. 1980. *Escherichia coli* mutator mutants deficient in
781 methylation-instructed DNA mismatch correction. *Proc Natl Acad Sci U S A*
782 **77**:1063–1067.
783 Goerke C, Pantucek R, Holtfreter S, Schulte B, Zink M, Grumann D, Bröker BM, Doskar
784 J, Wolz C. 2009. Diversity of prophages in dominant *Staphylococcus aureus* clonal
785 lineages. *J Bacteriol* **191**:3462–3468.
786 Goffin C, Ghuysen JM. 1998. Multimodular penicillin-binding proteins: an enigmatic
787 family of orthologs and paralogs. *Microbiol Mol Biol Rev* **62**:1079–1093.

bioRxiv preprint doi: https://doi.org/10.1101/2020.06.07.138933; this version posted June 7, 2020. The copyright holder for this preprint (which was not certified by peer review) is the author/funder, who has granted bioRxiv a license to display the preprint in perpetuity. It is made available under aCC-BY 4.0 International license.

788 Hershberg R. 2015. Mutation—the engine of evolution: studying mutation and its role in
789 the evolution of bacteria. *Cold Spring Harbor perspectives in*.
790 Hershberg R, Petrov DA. 2010. Evidence that mutation is universally biased towards AT
791 in bacteria. *PLoS Genet* **6**:e1001115.
792 Hidayat LK, Hsu DI, Quist R, Shriner KA, Wong-Beringer A. 2006. High-dose
793 vancomycin therapy for methicillin-resistant *Staphylococcus aureus* infections:
794 efficacy and toxicity. *Arch Intern Med* **166**:2138–2144.
795 Hildebrand F, Meyer A, Eyre-Walker A. 2010. Evidence of selection upon genomic GC-
796 content in bacteria. *PLoS Genet* **6**:e1001107.
797 Hiramatsu K. 2001. Vancomycin-resistant *Staphylococcus aureus*: a new model of
798 antibiotic resistance. *Lancet Infect Dis* **1**:147–155.
799 Hiramatsu K, Aritaka N, Hanaki H, Kawasaki S, Hosoda Y, Hori S, Fukuchi Y,
800 Kobayashi I. 1997. Dissemination in Japanese hospitals of strains of
801 *Staphylococcus aureus* heterogeneously resistant to vancomycin. *Lancet*
802 **350**:1670–1673.
803 Howden BP, Davies JK, Johnson PDR, Stinear TP, Grayson ML. 2010. Reduced
804 vancomycin susceptibility in *Staphylococcus aureus*, including vancomycin-
805 intermediate and heterogeneous vancomycin-intermediate strains: Resistance
806 mechanisms, laboratory detection, and clinical implications. *Clin Microbiol Rev*
807 **23**:99–139.
808 Howden BP, McEvoy CRE, Allen DL, Chua K, Gao W, Harrison PF, Bell J, Coombs G,
809 Bennett-Wood V, Porter JL, Robins-Browne R, Davies JK, Seemann T, Stinear TP.
810 2011. Evolution of multidrug resistance during *Staphylococcus aureus* infection

bioRxiv preprint doi: https://doi.org/10.1101/2020.06.07.138933; this version posted June 7, 2020. The copyright holder for this preprint (which was not certified by peer review) is the author/funder, who has granted bioRxiv a license to display the preprint in perpetuity. It is made available under aCC-BY 4.0 International license.

involves mutation of the essential two component regulator WalKR. *PLoS Pathog* **7**:e1002359.

Howden BP, Smith DJ, Mansell A, Johnson PDR, Ward PB, Stinear TP, Davies JK. 2008. Different bacterial gene expression patterns and attenuated host immune responses are associated with the evolution of low-level vancomycin resistance during persistent methicillin-resistant *Staphylococcus aureus* bacteraemia. *BMC Microbiology*. doi:10.1186/1471-2180-8-39

Howe RA, Bowker KE, Walsh TR, Feest TG, MacGowan AP. 1998. Vancomycin-resistant *Staphylococcus aureus*. *Lancet*.

Hu J, Zhang X, Liu X, Chen C, Sun B. 2015. Mechanism of reduced vancomycin susceptibility conferred by *walK* mutation in community-acquired methicillin-resistant *Staphylococcus aureus* strain MW2. *Antimicrob Agents Chemother* **59**:1352–1355.

Hu Q, Peng H, Rao X. 2016. Molecular events for promotion of vancomycin resistance in vancomycin intermediate *Staphylococcus aureus*. *Front Microbiol* **7**. doi:10.3389/fmicb.2016.01601

Ishii K, Tabuchi F, Matsuo M, Tatsuno K, Sato T, Okazaki M, Hamamoto H, Matsumoto Y, Kaito C, Aoyagi T, Hiramatsu K, Kaku M, Moriya K, Sekimizu K. 2015. Phenotypic and genomic comparisons of highly vancomycin-resistant *Staphylococcus aureus* strains developed from multiple clinical MRSA strains by in vitro mutagenesis. *Sci Rep* **5**:17092.

Jousselin A, Manzano C, Biette A, Reed P, Pinho MG, Rosato AE, Kelley WL, Renzoni A. 2015. The *Staphylococcus aureus* Chaperone PrsA Is a New Auxiliary Factor of

bioRxiv preprint doi: https://doi.org/10.1101/2020.06.07.138933; this version posted June 7, 2020. The copyright holder for this preprint (which was not certified by peer review) is the author/funder, who has granted bioRxiv a license to display the preprint in perpetuity. It is made available under aCC-BY 4.0 International license.

834 Oxacillin Resistance Affecting Penicillin-Binding Protein 2A. *Antimicrob Agents*
835 *Chemother* **60**:1656–1666.
836 Kato Y, Suzuki T, Ida T, Maebashi K. 2010. Genetic changes associated with
837 glycopeptide resistance in *Staphylococcus aureus*: predominance of amino acid
838 substitutions in YvqF/VraSR. *J Antimicrob Chemother* **65**:37–45.
839 Kumaraswamy M, Lin L, Olson J, Sun C-F, Nonejuie P, Corriden R, Döhrmann S, Ali
840 SR, Amaro D, Rohde M, Pogliano J, Sakoulas G, Nizet V. 2016. Standard
841 susceptibility testing overlooks potent azithromycin activity and cationic peptide
842 synergy against MDR *Stenotrophomonas maltophilia*. *J Antimicrob Chemother*
843 **71**:1264–1269.
844 Kuroda M, Kuroda H, Oshima T, Takeuchi F, Mori H, Hiramatsu K. 2003. Two-
845 component system VraSR positively modulates the regulation of cell-wall
846 biosynthesis pathway in *Staphylococcus aureus*. *Mol Microbiol* **49**:807–821.
847 Langmead B, Salzberg SL. 2012. Fast gapped-read alignment with Bowtie 2. *Nat*
848 *Methods* **9**:357–359.
849 Łęski TA, Tomasz A. 2005. Role of Penicillin-Binding Protein 2 (PBP2) in the Antibiotic
850 Susceptibility and Cell Wall Cross-Linking of *Staphylococcus aureus*: Evidence for
851 the Cooperative Functioning of PBP2, PBP4, and PBP2A. *J Bacteriol* **187**:1815–
852 1824.
853 Levine DP. 2006. Vancomycin: a history. *Clin Infect Dis* **42 Suppl 1**:S5–12.
854 Li B, Qiu Y, Shi H, Yin H. 2016. The importance of lag time extension in determining
855 bacterial resistance to antibiotics. *Analyst* **141**:3059–3067.
856 Lin L, Nonejuie P, Munguia J, Hollands A, Olson J, Dam Q, Kumaraswamy M, Rivera H

bioRxiv preprint doi: https://doi.org/10.1101/2020.06.07.138933; this version posted June 7, 2020. The copyright holder for this preprint (which was not certified by peer review) is the author/funder, who has granted bioRxiv a license to display the preprint in perpetuity. It is made available under aCC-BY 4.0 International license.

Jr, Corriden R, Rohde M, Hensler ME, Burkart MD, Pogliano J, Sakoulas G, Nizet V. 2015. Azithromycin Synergizes with Cationic Antimicrobial Peptides to Exert Bactericidal and Therapeutic Activity Against Highly Multidrug-Resistant Gram-Negative Bacterial Pathogens. *EBioMedicine* **2**:690–698.

Love MI, Huber W, Anders S. 2014. Moderated estimation of fold change and dispersion for RNA-seq data with DESeq. 2 Genome Biol 15: 550.

Machado H, Weng LL, Dillon N, Seif Y, Holland M, Pekar JE, Monk JM, Nizet V, Palsson BO, Feist AM. 2019. A defined minimal medium for systems analyses of *Staphylococcus aureus* reveals strain-specific metabolic requirements. *Appl Environ Microbiol* AEM–01773.

Marotz C, Amir A, Humphrey G, Gaffney J, Gogul G, Knight R. 2017. DNA extraction for streamlined metagenomics of diverse environmental samples. *Biotechniques* **62**:290–293.

Martens E, Demain AL. 2017. The antibiotic resistance crisis, with a focus on the United States. *J Antibiot* 1–7.

McAdam PR, Holmes A, Templeton KE, Fitzgerald JR. 2011. Adaptive evolution of *Staphylococcus aureus* during chronic endobronchial infection of a cystic fibrosis patient. *PLoS One* **6**:e24301.

McAleese F, Wu SW, Sieradzki K, Dunman P, Murphy E, Projan S, Tomasz A. 2006. Overexpression of Genes of the Cell Wall Stimulon in Clinical Isolates of *Staphylococcus aureus* Exhibiting Vancomycin-Intermediate- S. aureus-Type Resistance to Vancomycin. *Journal of Bacteriology*. doi:10.1128/jb.188.3.1120-1133.2006

bioRxiv preprint doi: https://doi.org/10.1101/2020.06.07.138933; this version posted June 7, 2020. The copyright holder for this preprint (which was not certified by peer review) is the author/funder, who has granted bioRxiv a license to display the preprint in perpetuity. It is made available under aCC-BY 4.0 International license.

McAleese F, Wu SW, Sieradzki K, Dunman P, Murphy E, Projan S, Tomasz A. 2006. Overexpression of genes of the cell wall stimulon in clinical isolates of *Staphylococcus aureus* exhibiting vancomycin-intermediate-S. aureus-type resistance to vancomycin. *J Bacteriol* **188**:1120–1133.

McCallum N, Stutzmann Meier P, Heusser R, Berger-Bächi B. 2011. Mutational analyses of open reading frames within the *vraSR* operon and their roles in the cell wall stress response of *Staphylococcus aureus*. *Antimicrob Agents Chemother* **55**:1391–1402.

McKee TJ, Komarova SV. 2017. Is it time to reinvent basic cell culture medium? *Am J Physiol Cell Physiol* **312**:C624–C626.

Mitsakakis K, Kaman WE, Elshout G, Specht M, Hays JP. 2018. Challenges in identifying antibiotic resistance targets for point-of-care diagnostics in general practice. *Future Microbiol* **13**:1157–1164.

Mohamed ET, Wang S, Lennen RM, Herrgård MJ, Simmons BA, Singer SW, Feist AM. 2017. Generation of a platform strain for ionic liquid tolerance using adaptive laboratory evolution. *Microb Cell Fact* **16**:1–15.

Murakami K. 1994. Nucleotide sequence of the structural gene for the penicillin-binding protein 2 of *Staphylococcus aureus* and the presence of a homologous gene in other staphylococci. *FEMS Microbiology Letters*. doi:10.1016/0378-1097(94)90184-8

Mwangi MM, Wu SW, Zhou Y, Sieradzki K, de Lencastre H, Richardson P, Bruce D, Rubin E, Myers E, Siggia ED, Tomasz A. 2007. Tracking the in vivo evolution of multidrug resistance in *Staphylococcus aureus* by whole-genome sequencing. *Proc*

bioRxiv preprint doi: https://doi.org/10.1101/2020.06.07.138933; this version posted June 7, 2020. The copyright holder for this preprint (which was not certified by peer review) is the author/funder, who has granted bioRxiv a license to display the preprint in perpetuity. It is made available under aCC-BY 4.0 International license.

903 *Natl Acad Sci U S A* **104**:9451–9456.

904 Oku Y, Kurokawa K, Ichihashi N, Sekimizu K. 2004. Characterization of the

905 *Staphylococcus aureus mprF* gene, involved in lysinylation of phosphatidylglycerol.

906 *Microbiology* **150**:45–51.

907 Organization WH. 2014. Antimicrobial resistance: global report on surveillance. *Who* 8.

908 Pader V, Hakim S, Painter KL, Wigneshweraraj S, Clarke TB, Edwards AM. 2016.

909 *Staphylococcus aureus* inactivates daptomycin by releasing membrane

910 phospholipids. *Nature Microbiology* **2**. doi:10.1038/nmicrobiol.2016.194

911 Peschel A, Otto M, Jack RW, Kalbacher H, Jung G, Götz F. 1999. Inactivation of the dlt

912 Operon in *Staphylococcus aureus* Confers Sensitivity to Defensins, Protegrins, and

913 Other Antimicrobial Peptides. *J Biol Chem* **274**:8405–8410.

914 Phaneuf PV, Gosting D, Palsson BO, Feist AM. 2018. ALEdb 1.0: a database of

915 mutations from adaptive laboratory evolution experimentation. *Nucleic Acids Res*

916 1–8.

917 Podolsky SH. 2018. The evolving response to antibiotic resistance (1945–2018).

918 *Palgrave Communications* **4**:1–8.

919 Pollack LA, Srinivasan A. 2014. Core elements of hospital antibiotic stewardship

920 programs from the Centers for Disease Control and Prevention. *Clin Infect Dis* **59**

921 **Suppl 3**:S97–100.

922 Poudel S, Tsunemoto H, Seif Y, Sastry AV, Szubin R, Xu S, Machado H, Olson C,

923 Anand A, Pogliano J, Nizet V, Palsson B. 2020. Revealing 29 sets of independently

924 modulated genes in *Staphylococcus aureus*, their regulators and role in key

925 physiological responses. *bioRxiv*. doi:10.1101/2020.03.18.997296

bioRxiv preprint doi: https://doi.org/10.1101/2020.06.07.138933; this version posted June 7, 2020. The copyright holder for this preprint (which was not certified by peer review) is the author/funder, who has granted bioRxiv a license to display the preprint in perpetuity. It is made available under aCC-BY 4.0 International license.

926 Read TD, Petit RA 3rd, Yin Z, Montgomery T, McNulty MC, David MZ. 2018. USA300
927 *Staphylococcus aureus* persists on multiple body sites following an infection. *BMC*
928 *Microbiol* **18**:206.
929 Sabat AJ, Tinelli M, Grundmann H, Akkerboom V, Monaco M, Del Grosso M, Errico G,
930 Pantosti A, Friedrich AW. 2018. Daptomycin Resistant *Staphylococcus aureus*
931 Clinical Strain With Novel Non-synonymous Mutations in the mprF and vraS
932 Genes: A New Insight Into Daptomycin Resistance. *Front Microbiol* **9**:2705.
933 Sakoulas G, Eliopoulos GM, Moellering RC Jr, Wennersten C, Venkataraman L, Novick
934 RP, Gold HS. 2002. Accessory gene regulator (*agr*) locus in geographically diverse
935 *Staphylococcus aureus* isolates with reduced susceptibility to vancomycin.
936 *Antimicrob Agents Chemother* **46**:1492–1502.
937 Salazar MJ, Machado H, Dillon NA, Tsunemoto H, Szubin R, Dahesh S, Pogliano J,
938 Sakoulas G, Palsson BO, Nizet V, Feist AM. 2020. Genetic Determinants Enabling
939 Medium-Dependent Adaptation to Nafcillin in Methicillin-Resistant *Staphylococcus*
940 *aureus*. *mSystems*. doi:10.1128/msystems.00828-19
941 Shore AC, Brennan OM, Ehricht R, Monecke S, Schwarz S, Slickers P, Coleman DC.
942 2010. Identification and Characterization of the Multidrug Resistance Gene cfr in a
943 Panton-Valentine Leukocidin-Positive Sequence Type 8 Methicillin-Resistant
944 *Staphylococcus aureus* IVa (USA300) Isolate. *Antimicrobial Agents and*
945 *Chemotherapy*. doi:10.1128/aac.01113-10
946 Sieradzki K, Tomasz A. 1999. Gradual Alterations in Cell Wall Structure and Metabolism
947 in Vancomycin-Resistant Mutants of *Staphylococcus aureus*. *J Bacteriol* **181**:7566–
948 7570.

bioRxiv preprint doi: https://doi.org/10.1101/2020.06.07.138933; this version posted June 7, 2020. The copyright holder for this preprint (which was not certified by peer review) is the author/funder, who has granted bioRxiv a license to display the preprint in perpetuity. It is made available under aCC-BY 4.0 International license.

Sorrell TC, Packham DR, Shanker S, Foldes M, Munro R. 1982. Vancomycin therapy for methicillin-resistant *Staphylococcus aureus*. *Ann Intern Med* **97**:344–350.

Strahl H, Hamoen LW. 2010. Membrane potential is important for bacterial cell division. *Proc Natl Acad Sci U S A* **107**:12281–12286.

Tran PM, Feiss M, Kinney KJ, Salgado-Pabón W. 2019. ϕSa3mw Prophage as a Molecular Regulatory Switch of *Staphylococcus aureus* β-Toxin Production. *J Bacteriol* **201**. doi:10.1128/JB.00766-18

(u.s.) CFDCAP, Centers for Disease Control and Prevention (U.S.). 2019. Antibiotic resistance threats in the United States, 2019. doi:10.15620/cdc:82532

van Wamel WJB, Rooijakkers SHM, Ruyken M, van Kessel KPM, van Strijp JAG. 2006. The Innate Immune Modulators Staphylococcal Complement Inhibitor and Chemotaxis Inhibitory Protein of *Staphylococcus aureus* Are Located on -Hemolysin-Converting Bacteriophages. *Journal of Bacteriology*. doi:10.1128/jb.188.4.1310-1315.2006

Verkaik NJ, Benard M, Boelens HA, de Vogel CP, Nouwen JL, Verbrugh HA, Melles DC, van Belkum A, van Wamel WJB. 2011. Immune evasion cluster-positive bacteriophages are highly prevalent among human *Staphylococcus aureus* strains, but they are not essential in the first stages of nasal colonization. *Clinical Microbiology and Infection*. doi:10.1111/j.1469-0691.2010.03227.x

Vidaillac C, Gardete S, Tewhey R, Sakoulas G, Kaatz GW, Rose WE, Tomasz A, Rybak MJ. 2013. Alternative mutational pathways to intermediate resistance to vancomycin in methicillin-resistant *Staphylococcus aureus*. *J Infect Dis* **208**:67–74.

Villanueva M, García B, Valle J, Rapún B, Ruiz de Los Mozos I, Solano C, Martí M,

bioRxiv preprint doi: https://doi.org/10.1101/2020.06.07.138933; this version posted June 7, 2020. The copyright holder for this preprint (which was not certified by peer review) is the author/funder, who has granted bioRxiv a license to display the preprint in perpetuity. It is made available under aCC-BY 4.0 International license.

Penadés JR, Toledo-Arana A, Lasa I. 2018. Sensory deprivation in *Staphylococcus aureus*. *Nat Commun* **9**:523.

Wang QM, Peery RB, Johnson RB, Alborn WE, Yeh WK, Skatrud PL. 2001. Identification and characterization of a monofunctional glycosyltransferase from *Staphylococcus aureus*. *J Bacteriol* **183**:4779–4785.

Xia G, Wolz C. 2014. Phages of *Staphylococcus aureus* and their impact on host evolution. *Infect Genet Evol* **21**:593–601.

bioRxiv preprint doi: https://doi.org/10.1101/2020.06.07.138933; this version posted June 7, 2020. The copyright holder for this preprint (which was not certified by peer review) is the author/funder, who has granted bioRxiv a license to display the preprint in perpetuity. It is made available under aCC-BY 4.0 International license.

Table S1 - Minimum inhibitory concentration (MIC_{90}) of *S. aureus* starting strains and TALE-derived strains in the same environmental conditions used for tolerance evolution, CA-MHB or RPMI+. Post-TALE refers to the MIC_{90} of the population after 21.79 ± 2.08 passages ($9.41x10^{11}$ ± $9.84x10^{10}$ CCDs) in the media used for evolution, without vancomycin. The post-TALE evolution was performed in duplicate for each of the end-point clones.

	MIC_{90} (µg/mL) in CA-MHB			MIC_{90} (µg/mL) in RPMI+	
Strain	**Starting strain / TALE**	**post-TALE**	**Strain**	**Starting strain / TALE**	**post-TALE**
WT	1	-	**WT**	2	-
SVAM_A2	4	ND	**SVAR_A1**	4	ND
SVAM_A3	8	4 / 4	**SVAR_A2**	8-16	8 / 8
STM2	1	-	**SVAR_A3**	16	16 / 16
SVAM_A6	4-8	2-4 / 4	**SVAR_A10**	8	ND
SVAM_A7	8	4 / 4	**STR1**	2	-
SVAM_A8	4	ND	**SVAR_A4**	8-16	8 / 8
STM3	1	-	**SVAR_A5**	8-16	8-16 / 8
SVAM_A9	8	4 / 4	**SVAR_A11**	8	ND
SVAM_A10	8	2 / 2	**STR4**	4	-
SVAM_A11	4	ND	**SVAR_A7**	8-16	8 -16 / 16
SVAM_A12	8	4 / 4	**SVAR_A8**	8	ND
			SVAR_A12	8	8 / 8

bioRxiv preprint doi: https://doi.org/10.1101/2020.06.07.138933; this version posted June 7, 2020. The copyright holder for this preprint (which was not certified by peer review) is the author/funder, who has granted bioRxiv a license to display the preprint in perpetuity. It is made available under aCC-BY 4.0 International license.

Figure S1 – Characteristics of vancomycin TALE strains. (A) An image of a plate displaying hemolytic activity after 24 h incubation at 37 °C for starting strains and vancomycin TALE strains (B) Autolysis of whole cells of *S. aureus*. Mid-exponential-phase cultures were resuspended in 0.05 M Tris-HCl (pH 7.2) containing 0.05% Triton X-100 and were incubated at 30°C. Absorbance was measured every hour and percentage to initial absorbance calculated.

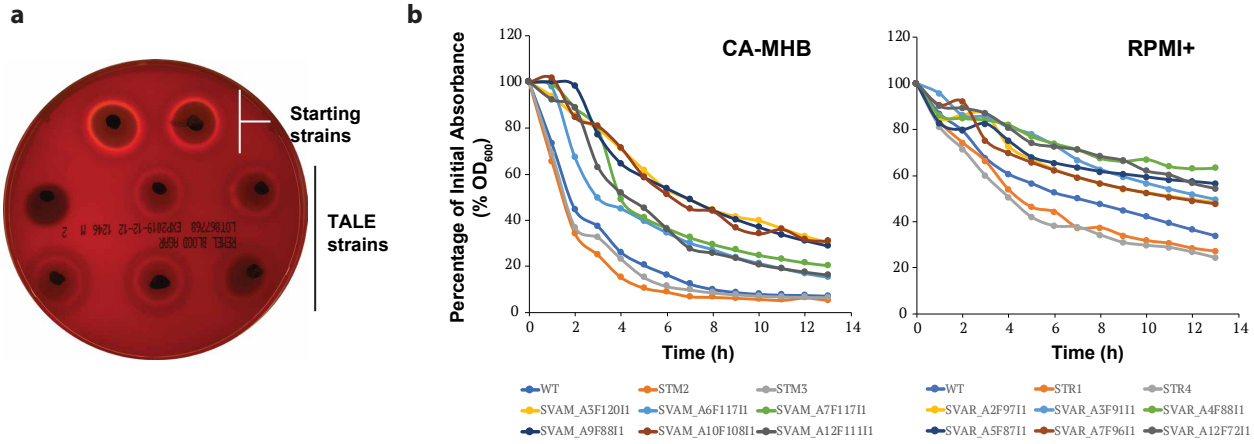

bioRxiv preprint doi: https://doi.org/10.1101/2020.06.07.138933; this version posted June 7, 2020. The copyright holder for this preprint (which was not certified by peer review) is the author/funder, who has granted bioRxiv a license to display the preprint in perpetuity. It is made available under aCC-BY 4.0 International license.

Table S2 – ANOVA statistical analysis of the lag-phase duration of starting strains and evolved strains in the same media as that used for tolerization.

vancomycin.ug.ml	Starting_strain	F.value	Pr..F.
0	STM2	4.37324747923248	0.062998644983095
0	STM3	8.21404843584888	0.0132439301947123
0	STR1	55.9776079042055	2.10636199647478E-05
0	STR4	18.2400821654054	0.00163482854999148
0.5	STM2	180.845045483513	9.94033084285709E-08
0.5	STM3	163.726248981813	9.6409038322023E-09
0.5	STR1	355.069596153815	3.83918455769995E-09
0.5	STR4	198.53651002671	6.36874197639287E-08
0	WT(MHB)	533.791403846887	7.21720540302604E-08
0	WT(RPMI)	11.7094080873006	0.00652657253351374
0.5	WT(MHB)	499.257469737133	9.09544723581264E-08
0.5	WT(RPMI)	5.55414886661091	0.0401771670140192

bioRxiv preprint doi: https://doi.org/10.1101/2020.06.07.138933; this version posted June 7, 2020. The copyright holder for this preprint (which was not certified by peer review) is the author/funder, who has granted bioRxiv a license to display the preprint in perpetuity. It is made available under aCC-BY 4.0 International license.

Figure S2 – Venn diagram of the key mutated genes (≥ 2 instances) in the two utilized media conditions (i.e., CA-MHB and RPMI+).